Apportionment of $PM_{2.5}$ and PM_{10} sources in the Richmond airshed, Tasman District

PK Davy WJ Trompetter

GNS Science Consultancy Report 2017/86
November 2017

GNS SCIENCE
TE PŪ AO

DISCLAIMER

This report has been prepared by the Institute of Geological and Nuclear Sciences Limited (GNS Science) exclusively for and under contract to Tasman District Council. Unless otherwise agreed in writing by GNS Science, GNS Science accepts no responsibility for any use of or reliance on any contents of this report by any person other than Tasman District Council and shall not be liable to any person other than Tasman District Council, on any ground, for any loss, damage or expense arising from such use or reliance.

Use of Data:

Date that GNS Science can use associated data: June 2017

BIBLIOGRAPHIC REFERENCE

Davy PK, Trompetter WJ. 2017. Apportionment of $PM_{2.5}$ and PM_{10} sources in the Richmond airshed, Tasman District. Lower Hutt (NZ): GNS Science. 69 p. (GNS Science consultancy report; 2017/86).

CONTENTS

FIGURES

TABLES

APPENDICES

APPENDIX FIGURES

EXECUTIVE SUMMARY

This report presents the results of a year-long (October 2015 to October 2016) daily $PM_{2.5}$ and multi-year PM_{10} (June 2013 to October 2016) sampling programme in Richmond. The particulate matter samples formed the basis of an elemental compositional analysis and identification of sources contributing to $PM_{2.5}$ and PM_{10} concentrations in the airshed while providing the opportunity to compare and confirm results from two independent datasets. The study builds upon two previous reports to Tasman District Council examining elemental concentrations in particulate matter and the sources contributing to air pollution in Richmond.

Key results from the study are:

1. Five main source types contributing to both $PM_{2.5}$ and PM_{10} were extracted from the data by receptor modelling techniques (using positive matrix factorisation), these were Biomass combustion, Motor vehicles, Secondary sulphate, Marine aerosol and a copper chromium, arsenic (CCA) source. Emissions from biomass combustion, attributed to solid fuel fires for home heating during the winter, were the primary source of both $PM_{2.5}$ and PM_{10} in the Richmond airshed and were also the dominant source contributing to exceedances of the PM_{10} National Environmental Standard for Air Quality (NES) of 50 $\mu g\ m^{-3}$.
2. On high pollution nights during winter, most of the particulate matter was in the fine fraction ($PM_{2.5}$) and it was found that there were many more days where $PM_{2.5}$ exceeded the New Zealand Ambient Air Quality Guideline (NZAAQG) of 25 $\mu g\ m^{-3}$ compared to PM_{10} NES exceedances.
3. The annual average arsenic concentrations in PM_{10} for the 2014 and 2015 calendar years, were 13 (±3) ng m^{-3}, and 16 (±3) ng m^{-3} respectively, significantly higher than the NZAAQG value of 5.5 ng m^{-3}. The long-term average (2013 to 2016) for arsenic was a similar value (14 ±3 ng m^{-3}). Elemental arsenic and lead in particulate matter were found to be strongly associated with the biomass combustion source with peaks in concentrations during winter. The arsenic and lead contamination was considered to be from the use of copper chrome arsenate treated timber and old painted timber respectively as fuel for domestic fires. A second source of arsenic associated with copper and chromium in $PM_{2.5}$ and PM_{10} was identified as a separate emission source to domestic solid fuel fires and was located northeast of the monitoring site.

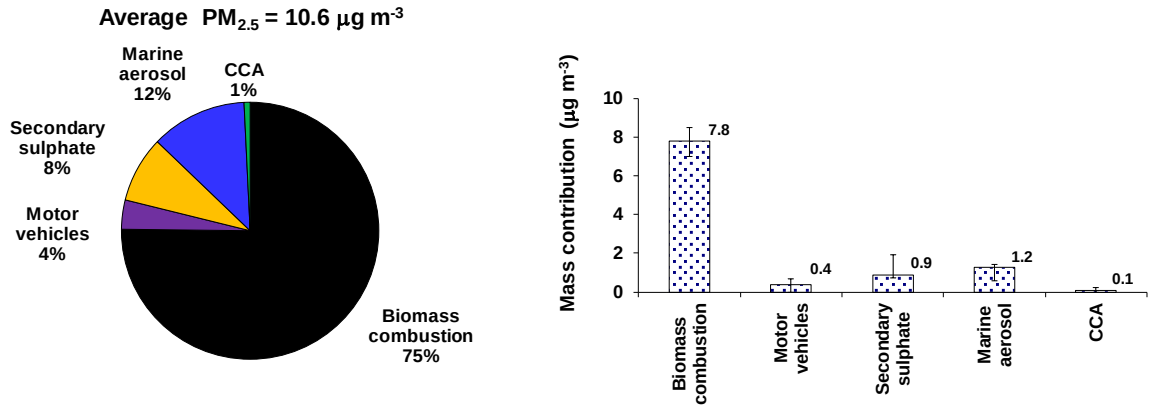

Figure ES1 Average source contributions to $PM_{2.5}$ in Richmond over the monitoring period (October 2015 – October 2016).

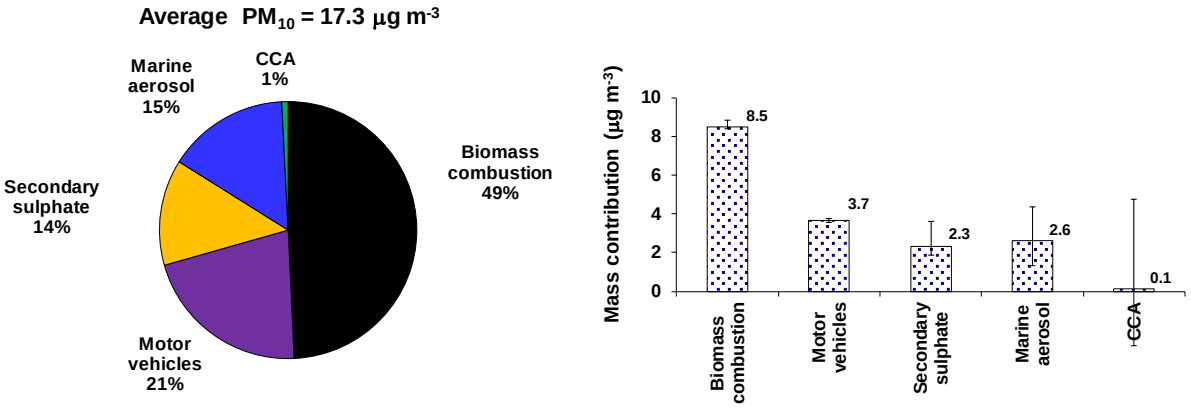

Figure ES2 Average source contributions to PM_{10} in Richmond over the monitoring period (June 2013 – October 2016).

1.0 INTRODUCTION

This report presents results from an investigation of $PM_{2.5}$ and PM_{10} sources using filter based samples collected at an ambient air quality monitoring site in Richmond, Tasman District. The current work follows on from a previous analysis of PM_{10} samples collected from June 2013 until September 2015 at the Richmond site (Ancelet and Davy 2016). In that report we identified the key sources driving peak PM_{10} concentrations and the natural background source contributions to assist with air quality management in the Richmond airshed. The focus of this work is on the finer $PM_{2.5}$ size fraction of particulate matter as Tasman District Council seeks to understand the sources that contribute to exceedances of the New Zealand Ambient Air Quality Guideline (NZAAQG) for $PM_{2.5}$ in anticipation of the current review of the National Environmental Standards for Air Quality (NESAQ) and the potential introduction of a mandatory $PM_{2.5}$ standard. However, the PM_{10} analysis has also been updated with an extra year of sampling in order to provide a comparison with the $PM_{2.5}$ results and examine the sources that contribute to the coarse ($PM_{10-2.5}$) particle fraction.

In Richmond $PM_{2.5}$ concentrations in excess of the NZAAQG (25 $\mu g/m^{-3}$) are measured regularly during the winter months (many more than for the PM_{10} NESAQ) which may present significant compliance and air quality management issues for Tasman District Council and therefore understanding the primary sources and their relative contributions to $PM_{2.5}$ concentrations is of major importance.

This work was commissioned by Tasman District Council (TDC) as part of their ambient air quality monitoring strategy and was partly funded by an Envirolink grant (C05X1608-TSDC131) from the Ministry of Business, Innovation and Employment.

The current report should be read in conjunction with the previous report on PM_{10} and the letter report examining the copper, chromium and arsenic constituents in $PM_{2.5}$ and PM_{10} samples from the Richmond monitoring site (Davy, P.K., *Elemental arsenic, copper and chromium concentrations at Richmond*, GNS Science Letter Report CR 2017/03 LR).

1.1 REQUIREMENT TO MANAGE AIRBORNE PARTICLE POLLUTION

In response to growing evidence of significant health effects associated with airborne particle pollution, the New Zealand Government introduced a National Environmental Standard (NES) in 2005 of 50 $\mu g\ m^{-3}$ for particles less than 10 µm in aerodynamic diameter (denoted as PM_{10}). The NES places an onus on regional councils to monitor PM_{10} and publicly report if the air quality in their region exceeds the standard. Initially, regional councils were required to comply with the standard by 2013 or face restrictions on the granting of resource consents for discharges that contain PM_{10}. However, the NES regulations were amended in April 2011 following a technical review, regulatory authorities are now required to comply by September 2016 with no more than three exceedances annually in airsheds such as Richmond and no more than one exceedance by September 2020 plus a provision for exceptional events (e.g. dust storms, volcanic eruptions) and a requirement for offsets by industry in PM_{10} polluted airsheds replacing the restriction on industrial consents (Ministry for the Environment. 2011. *Clean Healthy Air for All New Zealanders: National Air Quality Compliance Strategy to Meet the PM_{10} Standard*).

Clearly then, in areas where the PM_{10} standard is exceeded, information on the sources contributing to those air pollution episodes is required in order to:

- identify 'exceptional events' outside of regulatory authority control;
- effectively manage air quality and;
- formulate appropriate mitigation strategies where necessary.

In addition to the PM_{10} NES, the Ministry for the Environment issued ambient air quality guidelines for air pollutants in 2002 that included a (monitoring) guideline value of 25 $\mu g\ m^{-3}$ for $PM_{2.5}$ (24-hour average). More recently, the World Health Organisation (WHO) has confirmed a $PM_{2.5}$ ambient air quality guideline value of 25 $\mu g\ m^{-3}$ (24-hour average) based on the relationship between 24-hour and annual PM levels. The WHO annual average guideline for $PM_{2.5}$ is 10 $\mu g\ m^{-3}$. These are the lowest levels at which total, cardiopulmonary and lung cancer mortality have been shown to increase with more than 95% confidence in response to exposure to $PM_{2.5}$. WHO recommends the use of $PM_{2.5}$ guidelines over PM_{10} as epidemiological studies have shown that most of the adverse health effects associated with PM_{10} is due to $PM_{2.5}$.

1.2 IDENTIFYING THE SOURCES OF AIRBORNE PARTICLE POLLUTION

Measuring the mass concentration of particulate matter (PM) provides little or no information on the identities of the contributing sources. Airborne particles are composed of many elements and compounds emitted from various sources and a multivariate analysis technique known as receptor modelling allows the determination of relative mass contributions from sources impacting the total PM mass of samples collected at a monitoring site. First, gravimetric mass is measured and then a variety of methods can be used to determine the elements and compounds present in a sample. In this study, elemental concentrations in the samples were determined using X-ray fluorescence spectroscopy (XRF) at GNS Science in Lower Hutt.

X-ray fluorescence is a mature analytical technique that provides the non-destructive determination of multi-elemental concentrations in samples. Using elemental concentrations, coupled with appropriate statistical techniques and purpose-designed mathematical models, the sources contributing to each ambient sample can be identified. In general, the more ambient samples that are included in the analysis, the more robust the receptor modelling results. Appendix 1 provides a description of the XRF analytical process and receptor modelling techniques.

Several facets of air quality management have been addressed in the current work which has sought to:

- Identify and quantify elemental concentrations in $PM_{2.5}$ and PM_{10} including any toxic elements such as arsenic and lead;
- Identify the sources of toxic emissions;
- Identify and quantify those sources responsible for exceedances of the $PM_{2.5}$ NZAAQG and the PM_{10} NES;
- Examine seasonal differences in source contributions;
- Examine source contributions to $PM_{2.5}$ with wind speed and direction;
- Identify and quantify the mass contribution to $PM_{2.5}$ and PM_{10} from natural sources and other sources that are difficult or impossible to quantify by emissions inventories.
- Compare and contrast differences in elemental concentrations in, and source contributions to, $PM_{2.5}$ and PM_{10}.

At the same time the data was examined for exceptional events (i.e. exceedances of PM_{10}) that might fall outside the control of TDC.

1.3 REPORT STRUCTURE

This report is comprised of 6 main chapters. The remaining chapters have been broken down as follows:

- Chapter 2 describes the methodology and analytical techniques used for the receptor modeling analysis.
- Chapter 3 describes the Richmond ambient air quality monitoring site, temporal trends in PM_{10} concentrations and local meteorology.
- Chapter 4 presents the receptor modeling results for $PM_{2.5}$ and PM_{10}, including temporal variations and seasonality.
- Chapter 5 presents a discussion of the receptor modeling results.
- Chapter 6 provides a brief summary of the key results.

2.0 METHODOLOGY

$PM_{2.5}$ samples were collected onto Teflon filters on a daily basis using a sequential Partisol sampler located at 56 Oxford Street in Richmond. At the same time PM_{10} samples were also being collected alongside on a one-day-in-six basis. Figure 2.1 presents the location of the monitoring site. The monitoring site also featured an FH62 beta attenuation monitor (BAM) measuring PM_{10} concentrations continuously and a meteorological station collecting parameters such as wind speed and direction and ambient temperature. All PM sampling and systems maintenance at the sampling site was carried out by TDC, and as such, TDC maintains all records of equipment, flow rates and sampling methodologies used for the PM sampling regimes. Filter conditioning, weighing and re-weighing for PM_{10} gravimetric mass determinations were carried out by Watercare Services Limited.

Figure 2.1 Location of the Oxford Street monitoring site in Richmond (★) (source: Google Maps).

Elemental concentrations in PM_{10} were determined using X-ray fluorescence spectroscopy (XRF) at the New Zealand Ion Beam Analysis Facility in Gracefield, Lower Hutt. Black carbon (BC) concentrations were determined using light reflection techniques. Full descriptions of the analytical techniques used in this study are provided in Appendix 1.

The authors have been provided with information about the monitoring site and have been informed of the typical activities in the surrounding areas that may contribute to PM_{10} concentrations. These details informed the conceptual receptor model described in Chapter 3.

2.1 RECEPTOR MODELLING PROCESS

The multivariate analysis of air particulate matter sample composition (also known as receptor modelling) provides groupings (or factors) of elements that vary together over time. This technique effectively 'fingerprints' the sources that are contributing to airborne particulate matter and the mass of each element (and the PM mass) attributed to that source. In this study the primary source contributors were determined using results from the Positive Matrix Factorisation (PMF analysis) of the particulate matter elemental composition.

A critical point for understanding the receptor modelling process is that the PMF model can produce any number of solutions, all of which may be mathematically correct (Paatero, Hopke et al. 2002). The “best” solution (eg., number of factors, etc.) is generally determined by the practitioner after taking into account the model diagnostics and a review of the available factor profiles and contributions (to check physical interpretability). Most commonly used receptor models are based on conservation of mass from the point of emission to the point of sampling and measurement (Hopke 1999). Their mathematical formulations express ambient chemical concentrations as the sum of products of species abundances in source emissions and source contributions. In other words, the chemical profile measured at a monitoring station is resolved mathematically to be the sum of a number of different factors or sources. As with most modelling approaches, receptor models based on the conservation of mass are simplifications of reality and have the following general assumptions:

4. compositions of source emissions are constant over the period of ambient and source sampling;
5. chemical species do not react with each other (i.e., they add linearly);
6. all sources with a potential for contributing to the receptor have been identified and have had their emissions characterized;
7. the number of sources or source categories is less than or equal to the number of species measured;
8. the source profiles are linearly independent of each other; and
9. measurement uncertainties are random, uncorrelated, and normally distributed.

The effects of deviations from these assumptions are testable, and can therefore allow the accuracy of source quantification to be evaluated. Uncertainties in input data can also be propagated to evaluate the uncertainty of source contribution estimates. There are a number of natural physical restraints that must be considered when developing a model for identifying and apportioning sources of airborne particles, these are (Hopke 2003):

- the model must explain the observations;
- the predicted source compositions must be non-negative;
- the predicted source contributions must be non-negative;
- the sum of predicted elemental mass contributions from each source must be less than or equal to measured mass for each element.

These constraints need to be kept in mind when conducting and interpreting any receptor modelling approach, particularly since a receptor model is still an approximation of the real-world system. A number of factors also affect the nature of a sources’ particle composition and its contributions to ambient loadings (Brimblecombe 1986, Hopke 1999, Seinfeld and Pandis 2006):

1. the composition of particles emitted from a source may vary over time;
2. the composition of particles is modified in the atmosphere through a multitude of processes and interactions, for example;
    - adsorption of other species onto particle surfaces;
    - gas to particle conversions forming secondary particulate matter, for example the conversion of SO_2 gas to SO_4^{2-};
    - volatilisation of particle components such as organic compounds or volatilisation of Cl through reaction with acidic species;
    - interaction with and transformation by, solar radiation and free radicals in the atmosphere such as the OH and NO_3 species.

The analytical processes used in this study did not analyse for ammonium nitrate (elemental hydrogen, oxygen and nitrogen are not detectable by XRF techniques) so the missing mass that the analysis was not explaining is likely a combination of nitrate and other unmeasured species that are non-covariant (I.e. from the same sources) as those species that were measured. Analysis of ammonium nitrate aerosol in PM at other New Zealand locations suggests that the nitrate content (as NH_4NO_3) contributes approximately 0.7-1 µg m^{-3} to PM mass on average, most likely from a combination of urban emission sources (precursor gases such as NOx) and agricultural sources depending on location.

Analytical noise is also introduced during the species measurement process such as analyte interferences and limits of detection for species of interest. These are at least in the order of 5% for species well above its respective detection limit and 20% or more for those species near the analytical method detection limit (Hopke 1999). Further details on data analysis and dataset preparation are provided in Appendix 1.

Data Analysis and Reporting

The receptor modelling results within this report have been produced in a manner that provides as much information as possible on the relative contributions of sources to PM concentrations so that it may be used for monitoring strategies, air quality management and policy development. The data have been analysed to provide the following outputs:

1. masses of elemental species apportioned to each source;
2. source elemental profiles;
3. average PM_{10} mass apportioned to each source;
4. temporal variations in source mass contributions (timeseries plots);
5. seasonal variations in source mass contributions. For the purposes of this study, summer has been defined as December–February, autumn as March–May, winter as June–August and spring as September–November;
6. analysis of source contributions on peak PM days.

Table 2.1 presents the relevant standards, guidelines and targets for PM concentrations.

Table 2.1 Standards, guidelines and targets for PM concentrations.

Particle Size	Averaging Time	Ambient Air Quality Guideline	MfE* 'Acceptable' air quality category	National Environmental Standard
PM_{10}	24 hours	50 µg m^{-3}	33 µg m^{-3}	50 µg m^{-3}
	Annual	20 µg m^{-3}	13 µg m^{-3}	
$PM_{2.5}$	24 hours	25 µg m^{-3}	17 µg m^{-3}	

*Ministry for the Environment air quality categories taken from the Ministry for the Environment, October 1997 – ***Environmental Performance Indicators: Proposals for Air, Fresh Water and Land***.

3.0 OXFORD STREET MONITORING SITE AND SAMPLING METHODOLOGY

3.1 SITE DESCRIPTION

$PM_{2.5}$ and PM_{10} samples were collected at an ambient air quality monitoring station located at 56 Oxford street, Richmond (Lat: 41°20'21.46 S; Long: 173°10'58.65 E; elevation: 13 m). Figure 3.1 presents the site location on a map of the local area.

Figure 3.1 Map showing the location of the Oxford Street monitoring site (source: TDC).

Oxford Street is located near the Richmond CBD and the monitoring site was less than 400 m from State Highway 6, the major roadway into and out of Nelson. The site was in a residential area and was surrounded by buildings no higher than two stories. Aside from its immediate environment, the monitoring site was surrounded by hills and farmland, and was less than 5 km south of Tasman Bay.

3.2 PARTICULATE MATTER SAMPLING AND MONITORING PERIOD

In this study, 360 daily (midnight to midnight) $PM_{2.5}$ samples were collected between October 2015 and October 2016 using a sequential Partisol sampler. Additionally, PM_{10} samples were collected on a one-day-in-six (midnight to midnight) sampling regime, and were a continuation of the PM_{10} sampling for speciation analysis reported previously (i.e. beginning June 2013). Mass concentrations of PM_{10} and $PM_{2.5}$ were determined gravimetrically, where a filter of known weight was used to collect the PM samples from a known volume of sampled air. The loaded filters were then re-weighed to obtain the mass of collected PM. The average PM concentration in the sampled air was then calculated.

3.3 CONCEPTUAL RECEPTOR MODEL FOR PM_{10} IN RICHMOND

An important part of the receptor modeling process is to formulate a conceptual model of the receptor site. This means understanding and identifying the major sources that may influence ambient PM concentrations at the site. For the Richmond site, the initial conceptual model includes local emission sources:

- Motor vehicles – all roads in the area act as line sources, and roads with higher traffic densities and congestion will dominate;
- Domestic activities – likely to be dominated by biomass combustion activities like emissions from solid fuel fires used for domestic heating during the winter;
- Local wind-blown soil or road dust sources may also contribute.

Sources that originate further from the monitoring site would also be expected to contribute to ambient particle loadings, and these include:

- Marine aerosol;
- Secondary PM resulting from atmospheric gas-to-particle conversion processes – includes sulphates, nitrates and organic species;
- Potential industrial emissions from combustion processes (boilers) and dust generating activities;
- Emissions from ships in the Port area of Nelson.

Another category of emission sources that may contribute are those considered to be ‘one-off’ emission sources:

- Fireworks displays and other special events (e.g. Guy Fawkes day);
- Short-term road works and demolition/construction activities.

The variety of sources described above can be recognised and accounted for using appropriate data analysis methods such as examination of seasonal differences, temporal variations and receptor modeling itself.

3.4 LOCAL METEOROLOGY IN RICHMOND

A meteorological station was located on the roof of the Tasman District Council (TDC) building at 189 Queen Street approximately 300 m from the PM monitoring site. The meteorological station is owned and operated by TDC. As shown in Figure 3.2, the predominant wind directions were from the southwest and north/northeast. Winds from other directions were uncommon. Some seasonality was apparent in wind speeds, with speeds lower during winter and stronger winds from the north-northeast during summer, but no seasonality was apparent for wind directions (Figure 3.3).

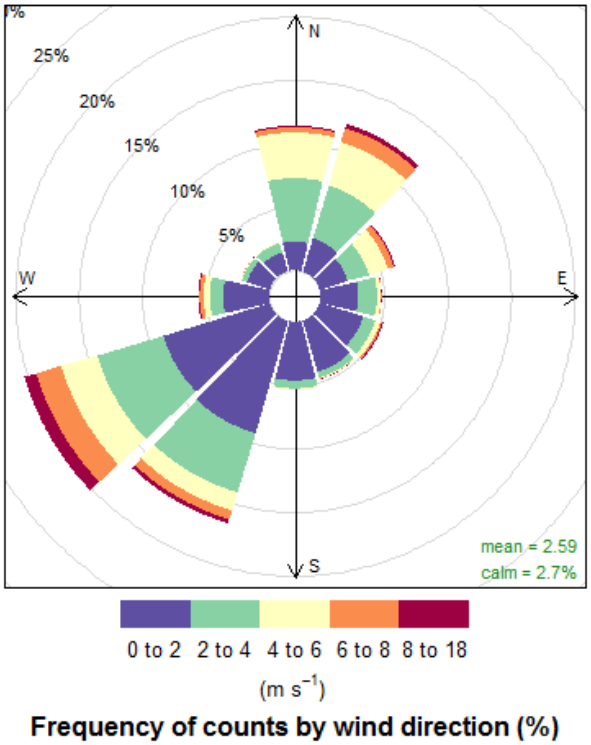

Figure 3.2 Wind rose for the entire monitoring period (June 2013 – October 2016).

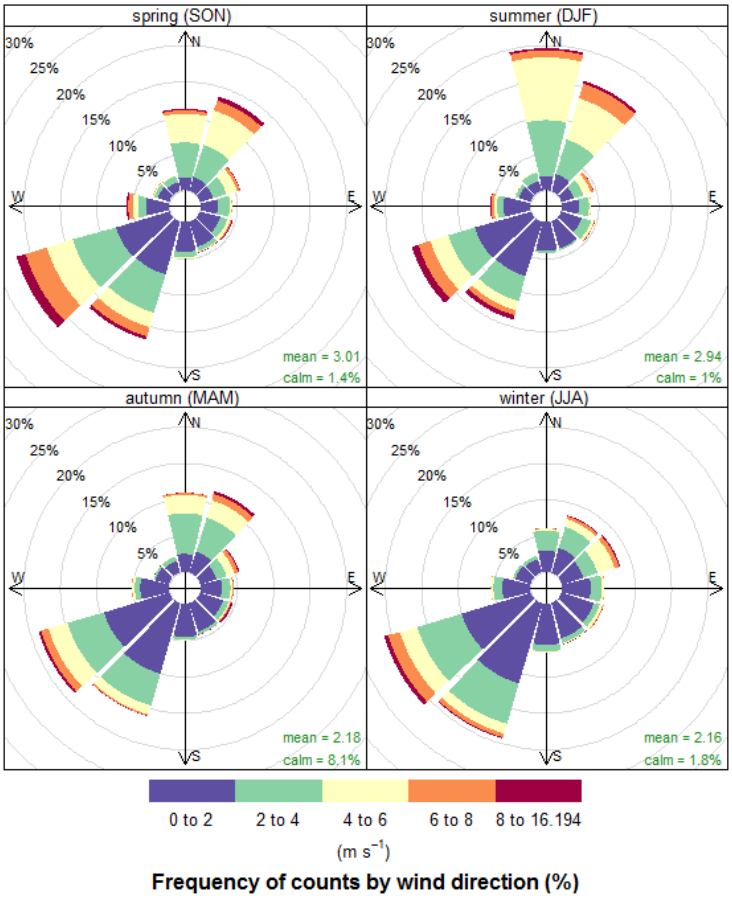

Figure 3.3 Wind roses by season over the entire monitoring period (June 2013 – October 2016).

3.5 PM_{10} CONCENTRATIONS IN RICHMOND

PM_{10} concentrations were continuously monitored at the Richmond site using a Thermo-Anderson FH62 Beta-particle Attenuation Monitor (BAM) operated according to AS/NZS 3580.9.11.2008. Figure 3.4 presents the BAM PM_{10} monitoring results (midnight to midnight) over the monitoring period (June 2013–October 2016). Figure 3.4 shows that PM_{10} concentrations in Richmond have seasonal patterns, with concentrations peaking during winter. Gaps present in Figure 3.4 are from sampler outages (malfunction/maintenance). Between 2013 and 2016, the PM_{10} NES was exceeded eighteen times in Richmond[1].

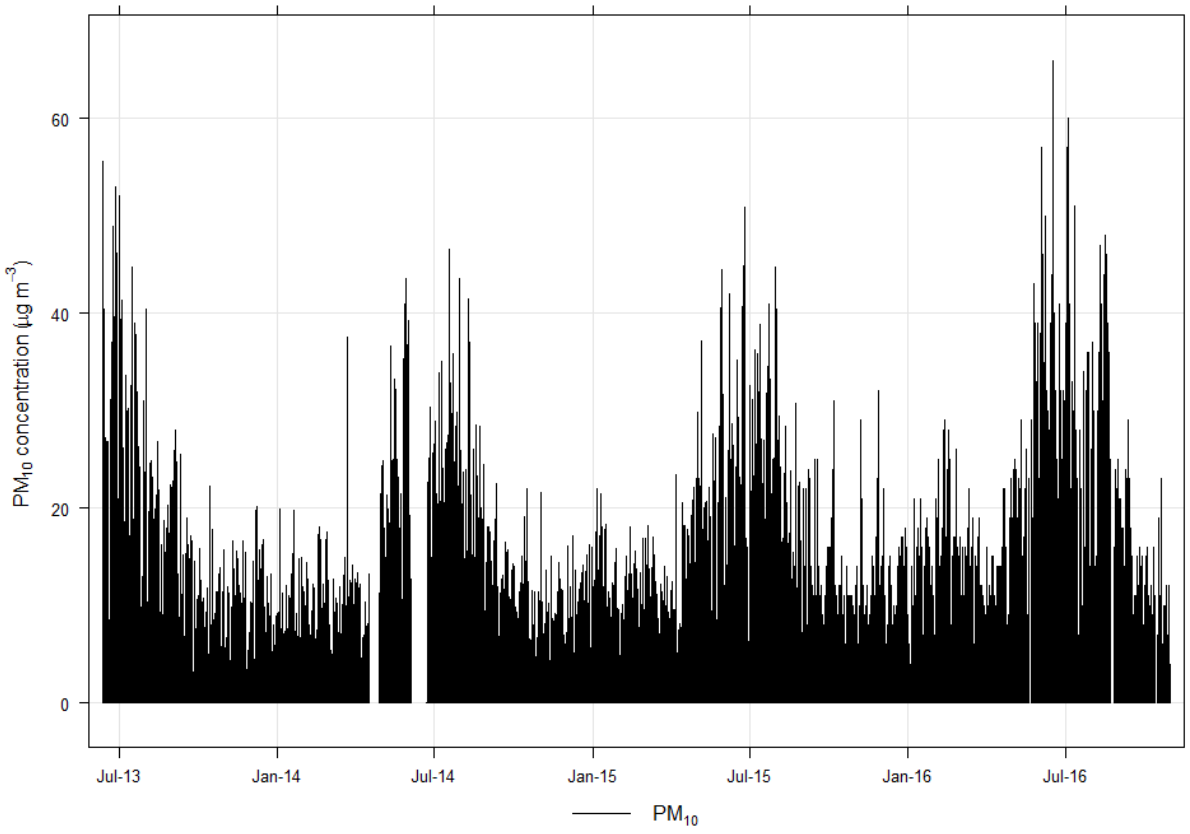

Figure 3.4 PM_{10} (BAM 24-hour average) concentrations in Richmond (data supplied by TDC).

[1] (http://www.tasman.govt.nz/environment/air/air-quality/).

4.0 RECEPTOR MODELING ANALYSIS OF $PM_{2.5}$ AND PM_{10} IN RICHMOND

4.1 ANALYSIS OF $PM_{2.5}$ SAMPLES COLLECTED AT RICHMOND

$PM_{2.5}$ samples in Richmond were collected using a sequential Partisol sampler system, on a daily (midnight to midnight) sampling regime. Overall, 357 samples were collected from October 2015 to October 2016. $PM_{2.5}$ concentrations were determined gravimetrically and elemental and BC concentrations were determined using XRF and light reflection, respectively, as described in Appendix 1. Gravimetric results for the $PM_{2.5}$ samples are presented in Figure 4.1. A clear seasonal pattern is apparent from Figure 4.1, with $PM_{2.5}$ concentrations peaking from May–August. Outside of the winter season, $PM_{2.5}$ concentrations were relatively low. Gaps present in Figure 4.1 resulted from missed sample days or samples removed as part of the quality assurance process, which could include, but would not be limited to, routine maintenance or equipment failure.

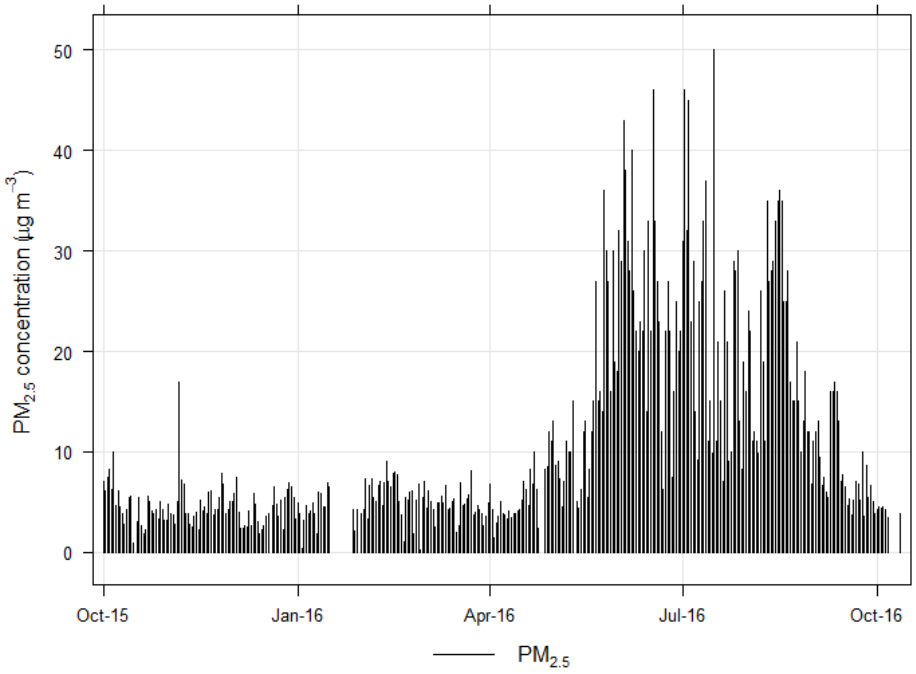

Figure 4.1 Gravimetric $PM_{2.5}$ results from the Richmond monitoring site. Gaps are from missed sample days or samples removed as part of the quality assurance process.

4.1.1 Composition of $PM_{2.5}$ at Richmond

Elemental concentrations in the samples collected are presented in Table 4.1. Table 4.1 indicates that some measured species were close to or below their respective limit of detection (LOD) in each of the samples. Carbonaceous species, represented by BC, were found to dominate $PM_{2.5}$ mass concentrations. Along with BC, other important elemental constituents included Na, Cl, and K indicating that combustion sources, and marine aerosol particles are important contributors to PM_{10} concentrations at the monitoring site. An elemental correlation plot is provided in Figure A2.1 in Appendix 2.

Table 4.1 also shows that some of the heavy metal elements are present at significant concentrations above their respective LOD, particularly for arsenic and lead. Figure 4.2 presents the temporal variation for arsenic and lead showing a winter peak for both contaminants. Arsenic concentrations also had some significant non-winter peaks as found for PM_{10} in the previous study (Ancelet and Davy 2016). When examined in conjunction with the elemental correlation plot in Appendix 2 it shows that arsenic and lead concentrations are correlated with black carbon suggesting that they are associated with combustion sources.

Table 4.1 Elemental concentrations in $PM_{2.5}$ samples from Richmond (357 samples).

	Average (ng m^{-3})	Maximum (ng m^{-3})	Minimum (ng m^{-3})	Median (ng m^{-3})	Std Dev (ng m^{-3})	Uncertainty (ng m^{-3})	LOD (ng m^{-3})	% > LOD
$PM_{2.5}$	**10600**	**50000**	**0**	**6000**	**10000**			
BC	2949	12279	8	1505	2868	231	159	99
Na	360	1633	5	296	264	157	141	80
Mg	97	713	0	93	57	17	5	96
Al	24	408	0	13	43	29	26	29
Si	37	706	0	21	70	27	25	45
P	1	11	0	0	2	14	20	0
S	166	931	2	148	92	31	21	100
Cl	360	2422	0	255	359	40	6	97
K	172	4714	0	101	282	21	5	100
Ca	19	250	0	15	22	7	6	83
Ti	3	32	0	2	3	6	5	11
V	0	33	0	0	2	4	4	1
Cr	8	137	0	2	17	3	2	42
Mn	2	16	0	1	2	3	2	39
Fe	30	303	1	25	26	6	2	100
Co	0	3	0	0	0	7	10	0
Ni	1	5	0	0	1	3	2	6
Cu	7	110	0	3	11	4	4	42
Zn	10	47	0	7	10	5	5	60
Ga	1	6	0	0	1	17	20	0
As	13	171	0	5	19	4	2	66
Se	0	8	0	0	1	21	31	0
Br	6	34	0	5	5	14	14	8
Sr	2	182	0	0	10	13	12	1
Y	0	5	0	0	1	12	17	0
Zr	2	11	0	0	2	24	25	0
Nb	1	9	0	0	2	22	21	0
Mo	1	11	0	0	2	27	28	0
Pd	2	20	0	0	4	16	14	1
Cd	2	14	0	0	3	22	17	0
Sn	3	20	0	2	4	24	20	0
Sb	2	20	0	0	4	19	19	1
Te	4	29	0	1	6	24	22	1
Cs	6	36	0	1	8	24	22	6
Ba	4	395	0	0	22	26	23	3
La	7	72	0	0	12	31	22	12
Ce	39	417	0	0	67	134	122	12
Sm	31	321	0	0	58	67	47	23
Pb	7	31	0	5	6	6	4	61

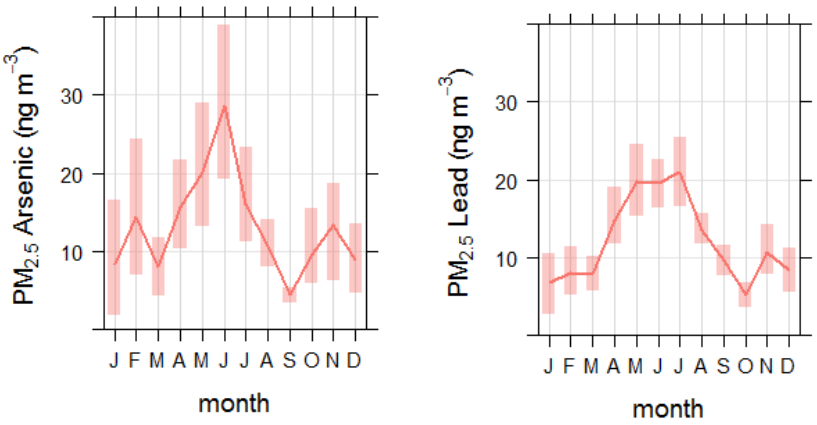

Figure 4.2 Temporal variation for arsenic (left); and lead (right) showing peak winter concentrations. Shaded areas represent the 95% confidence intervals.

The New Zealand ambient air quality guidelines (AAQG) provide guideline values (in PM_{10}) for arsenic (inorganic arsenic is 5.5 ng m^{-3} as an annual average) and lead (200 ng m^{-3} as a 3-month moving average, calculated monthly) (MfE 2002). Table 4.1 indicates that the (non-calendar year) annual average for arsenic in $PM_{2.5}$ was 13 (±3) ng m^{-3}. The 3-month moving average lead concentrations peaked during winter 2016 at around 20 ng m^{-3}, somewhat less than the AAQG of 200 ng m^{-3}.

Another source of peak elemental concentrations was associated with pyrotechnic events (fireworks) around the 5th November 2015 (Guy Fawkes). This is particularly evident for potassium, one of the main ingredients of gunpowder, along with copper (blue colour in fireworks) strontium (red colour in fireworks) and barium (green colour in fireworks) as presented in Figure 4.3. Note that there was also a peak in $PM_{2.5}$ (on 6 November 2015) that coincided with the pyrotechnics showing that such events can have an influence on ambient particulate matter concentrations.

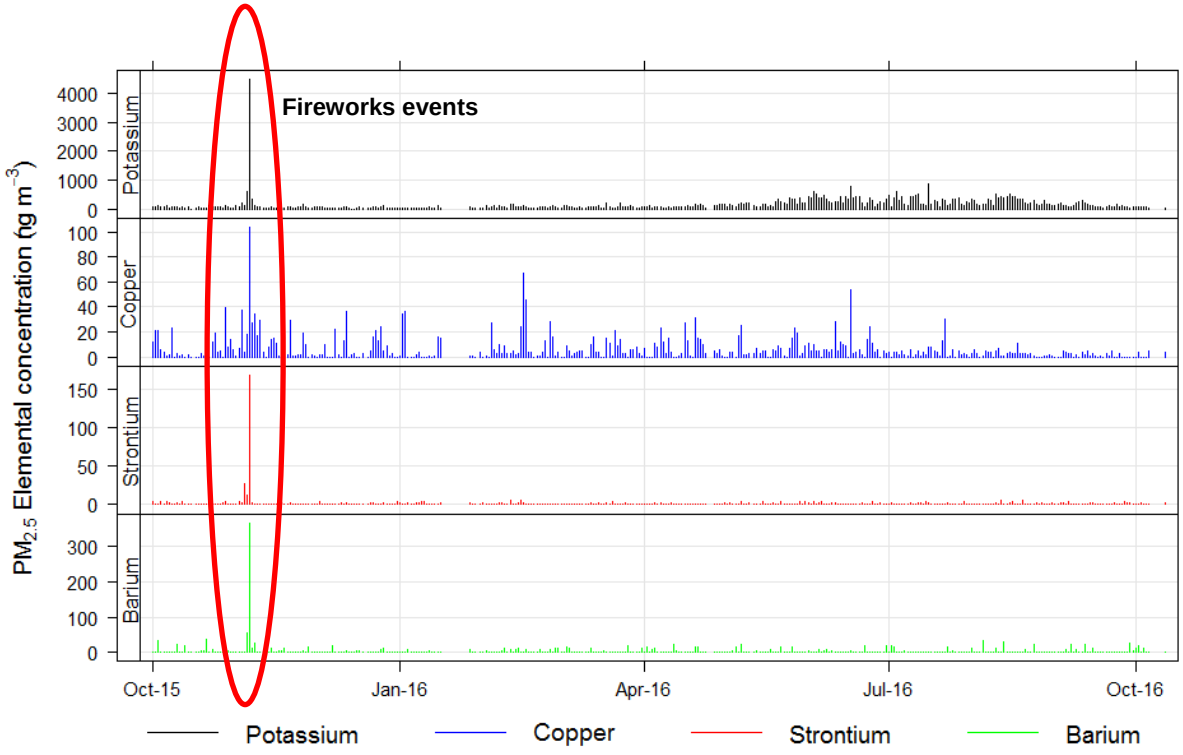

Figure 4.3 Timeseries for potassium, copper, strontium and barium at the Richmond site showing peak concentrations around 5 November 2015 associated with pyrotechnic events.

4.1.2 Source Contributions to $PM_{2.5}$ in Richmond

Five source contributors were identified from PMF receptor modeling analysis of the $PM_{2.5}$ data from Richmond. Table 4.2 and Figure 4.4 present the average elemental concentration source profiles extracted from the PMF analysis. The source contributors identified were found to explain 96% of the gravimetric PM_{10} mass on average.

The sources identified were:

- Biomass combustion: The first factor was identified as biomass combustion based on the dominance of BC and K in the profile (Fine, Cass et al. 2001, Khalil and Rasmussen 2003). Arsenic and Pb were strongly associated with the biomass combustion profile. This phenomenon is consistent throughout New Zealand and indicates that residents are burning copper chrome arsenate-treated and lead-painted timber, respectively (Ancelet et al. 2012);
- Motor vehicles: the second factor was identified as motor vehicles because of the presence of BC, Al, Si, Ca, Ti and Fe as significant elemental components. This profile is likely to be primarily a motor vehicle tailpipe (BC representing fuel combustion) emission source with some re-entrained road dust emissions (Al, Si, Ca, Ti, Fe as the crustal matter components);
- Secondary sulphate: the third factor was identified as secondary sulphate because of the dominance of S in the profile. This source contribution was likely to be associated with secondary sulphate aerosol produced in the atmosphere from gaseous precursors;
- Marine aerosol: the fourth factor was identified as a marine aerosol source because of the predominance of Na and Cl, along with some Mg, S, K, and Ca;
- CCA: the fifth factor was identified as originating from emissions of copper chrome arsenate containing particulate matter. This is a similar result as identified in the PM_{10} (June 2013 – September 2015) analysis. It was surmised in the previous PM_{10} study that the CCA source profile was likely to be associated with a point source discharge.

Table 4.2 Source elemental concentration profiles for $PM_{2.5}$ samples from Richmond.

	Biomass combustion (ng m^{-3})	Motor vehicles (ng m^{-3})	Secondary sulphate (ng m^{-3})	Marine aerosol (ng m^{-3})	CCA (ng m^{-3})
$PM_{2.5}$	7800	400	860	1200	100
BC	2496	276.7	36.0	74.6	34.5
Na	10.0	47.4	74.3	214.0	8.0
Al	0.1	19.5	0.0	0.2	0.1
Si	0.0	30.9	0.0	0.0	0.3
S	21.8	31.2	76.7	28.2	4.1
Cl	37.1	6.0	0.0	305.3	4.0
K	113.4	16.8	8.0	8.6	4.8
Ca	0.0	8.2	1.8	6.7	0.8
Ti	0.1	1.4	0.0	0.2	0.0
Cr	0.0	0.4	0.3	0.0	6.9
Fe	6.6	18.2	1.3	1.5	0.9
Cu	0.6	0.4	0.1	0.3	4.1
Zn	6.9	1.6	0.8	0.0	0.1
As	4.4	0.0	0.2	0.2	7.2
Pb	3.0	0.7	0.7	0.3	0.2

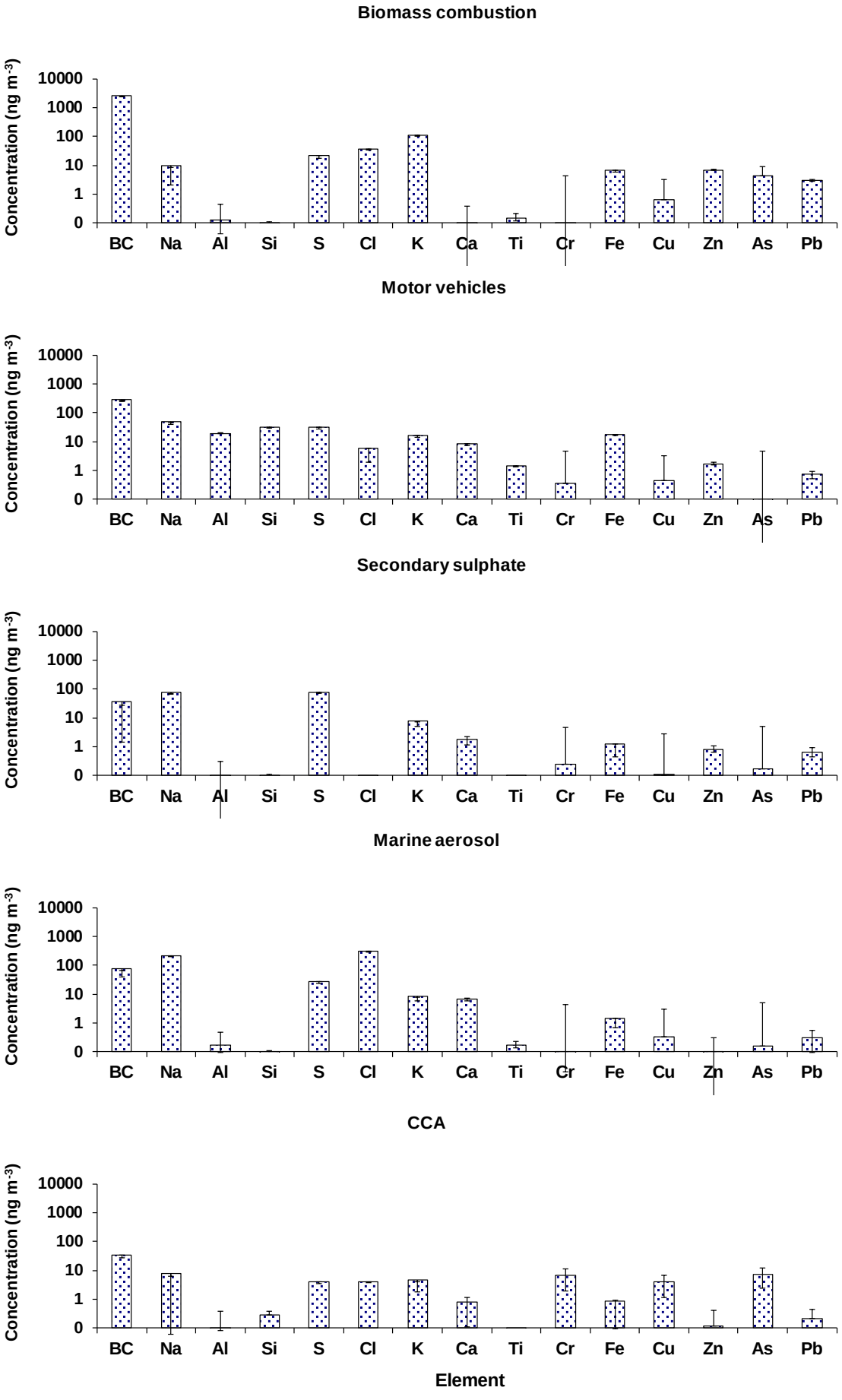

Figure 4.4 Source elemental concentration profiles for $PM_{2.5}$ samples from Richmond.

Figure 4.5 presents the relative source contributions to PM_{10} in Richmond. Also included in Figure 4.5 are the 5th and 95th percentile confidence limits in $PM_{2.5}$ mass attributed to each of the sources.

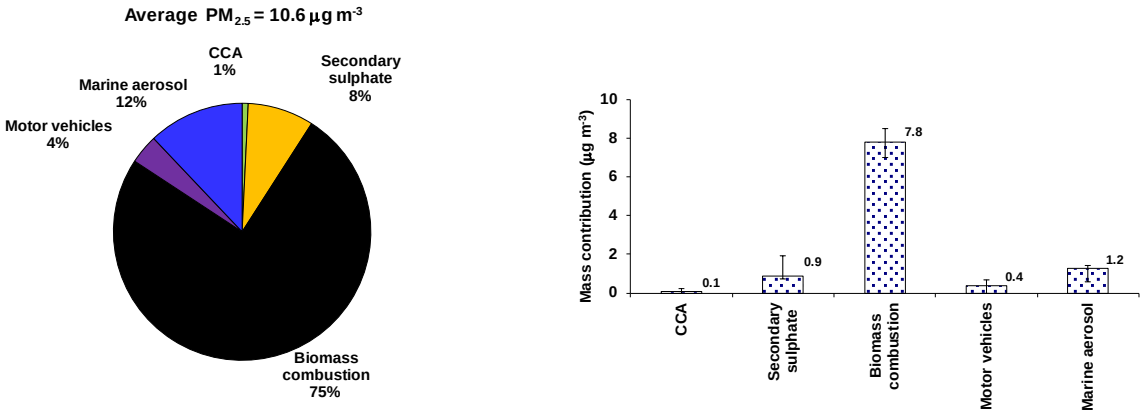

Figure 4.5 Average source contributions to $PM_{2.5}$ in Richmond over the monitoring period (September 2015 – October 2016).

The average $PM_{2.5}$ source contributions over the entire monitoring period estimated from the PMF analysis showed that biomass combustion was the most significant contributor to $PM_{2.5}$ mass (75%). Secondary sulphate (8%), marine aerosol (12%) and motor vehicles (4%) had lesser contributions to $PM_{2.5}$ mass, while CCA had the lowest (trace) contribution (1%).

Temporal variations in the source contributions are presented in Figure 4.6 (note the difference in concentration scales and that gaps in the data are due to missing sample periods). It was evident that $PM_{2.5}$ mass is dominated by the biomass combustion source during winter, which arises primarily from emissions from solid fuel fires used for domestic heating. During other time periods, marine aerosol, sulphate and motor vehicle contributions were the primary sources contributing to $PM_{2.5}$. The PM due to the CCA source was present intermittently at relatively low concentrations.

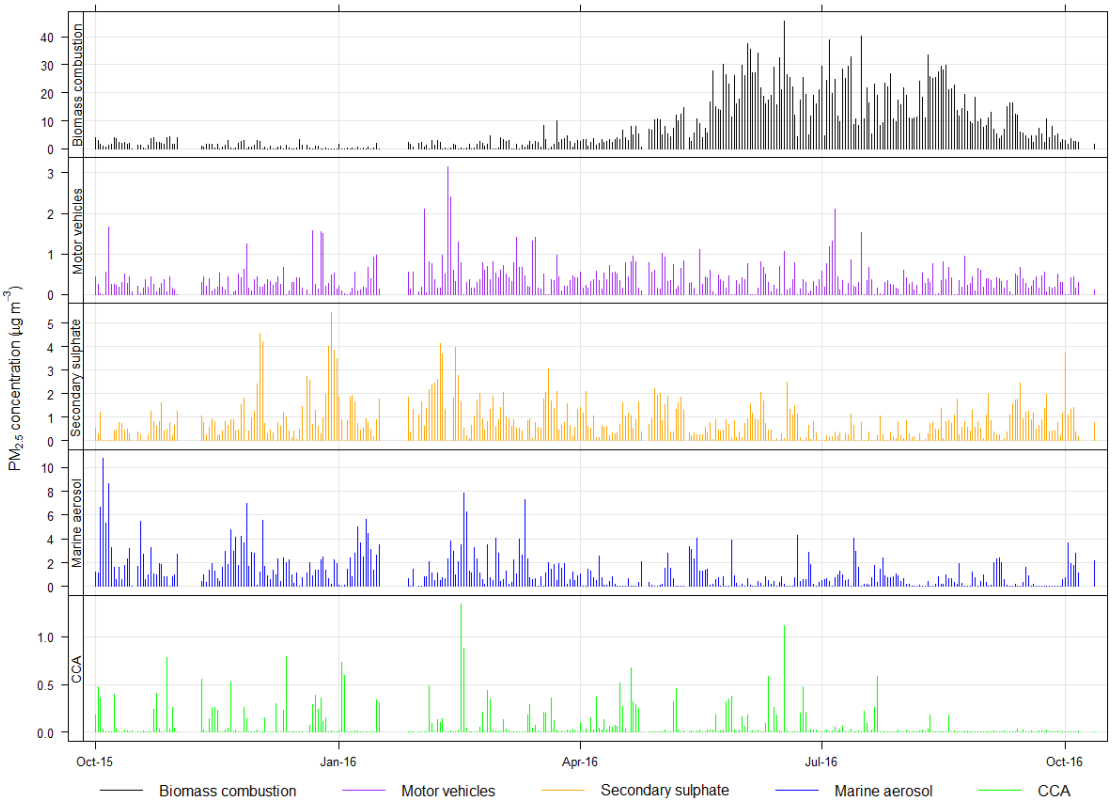

Figure 4.6 Temporal variations in relative source contributions to $PM_{2.5}$ mass.

4.1.3 Seasonal Variations in $PM_{2.5}$ Sources at Richmond

$PM_{2.5}$ was found to peak in Richmond from late Autumn until the end of winter (May to September). Figure 4.7 and Figure 4.8 present average monthly $PM_{2.5}$ concentrations and source contributions, respectively. The dominant source of $PM_{2.5}$ from May to September in Richmond was biomass combustion associated with solid fuel fire emissions for domestic heating and was clearly the driver of $PM_{2.5}$ concentrations over the same period. Some seasonality was apparent in the marine aerosol source, which peaked during spring and summer when wind speeds tend to increase. A distinct seasonality in concentrations was observed for the secondary sulphate source with peak summer concentrations in line with solar forcing of atmospheric chemistry coupled with source activity. Otherwise, little seasonality was apparent in the motor vehicle and CCA sources.

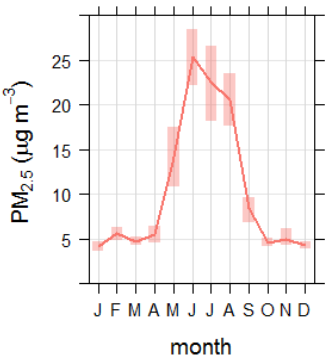

Figure 4.7 Average monthly $PM_{2.5}$ concentrations in Richmond. Shaded areas represent the 95% confidence intervals.

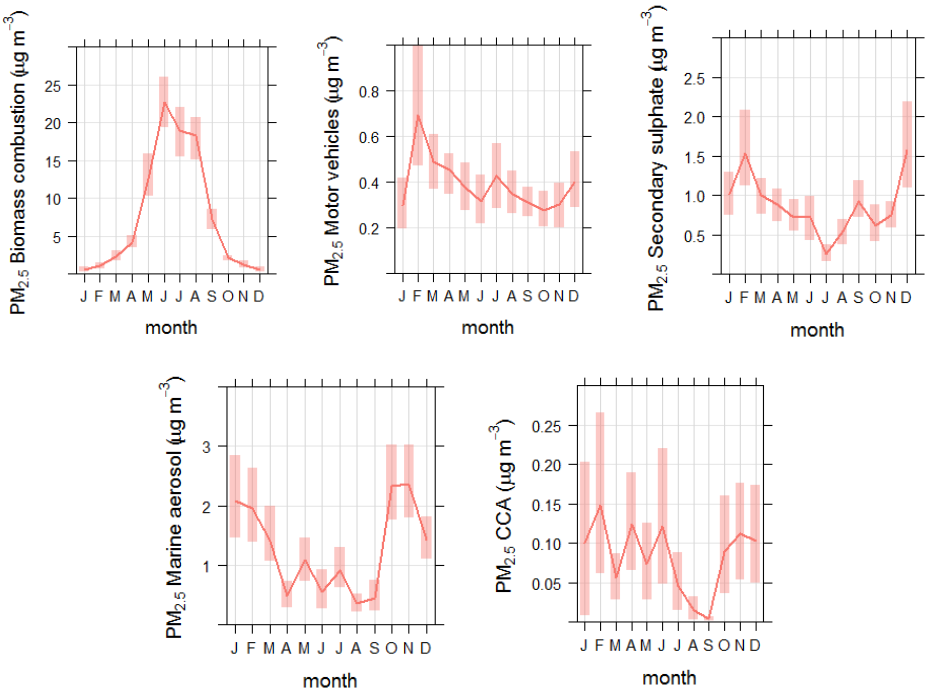

Figure 4.8 Average monthly source contributions to $PM_{2.5}$ in Richmond. Shaded areas represent the 95% confidence intervals.

4.1.4 Daily Variations in $PM_{2.5}$ Sources at Richmond

Source contributions to $PM_{2.5}$ concentrations were analysed by day of the week to investigate any potential weekday/weekend variations. Figure 4.9 presents $PM_{2.5}$ concentration variations by day of the week. It was evident that $PM_{2.5}$ concentrations were not statistically different day-to-day, and no weekday/weekend difference was apparent. However, analysis of source contributions revealed that the motor vehicle source contributions were significantly lower on weekends than weekdays (Figure 4.10), and is likely to be indicative of lower traffic densities during the weekend than weekdays associated with normal working week and commuter behaviour.

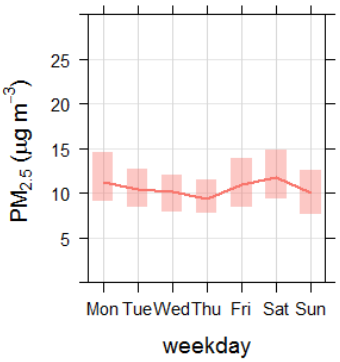

Figure 4.9 Variation in PM_{10} concentrations in Richmond by day of the week. Shaded areas represent the 95% confidence intervals.

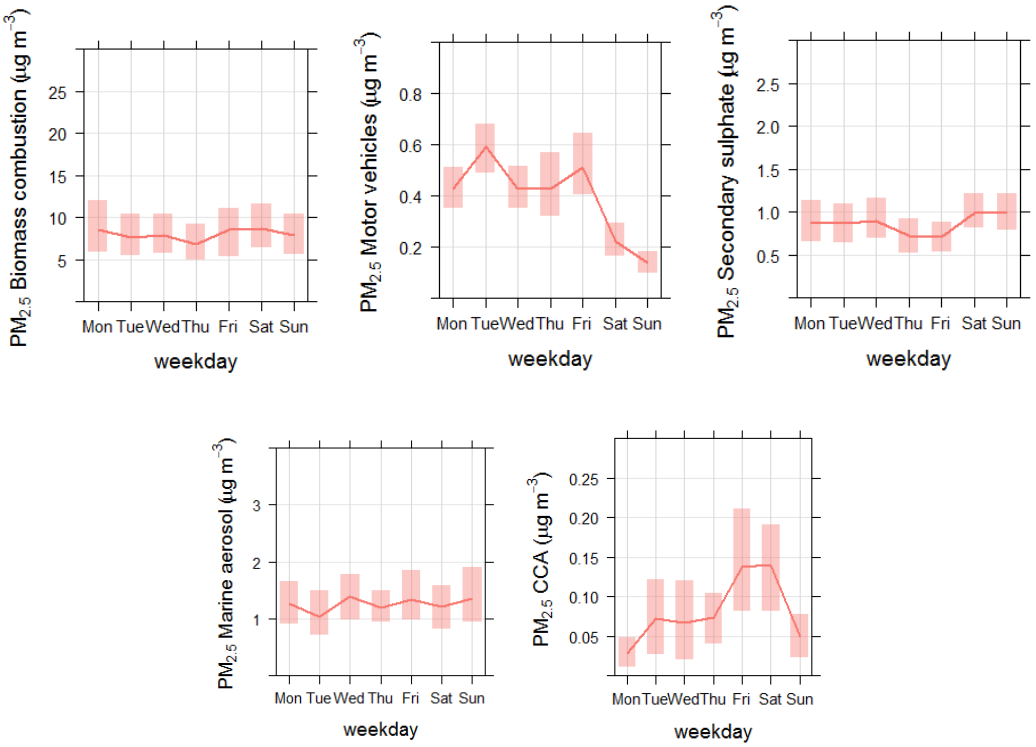

Figure 4.10 Variation in source contributions to $PM_{2.5}$ in Richmond by day of the week. Shaded areas represent the 95% confidence intervals.

4.2 ANALYSIS OF PM_{10} SAMPLES COLLECTED AT RICHMOND

PM_{10} samples from Richmond previously been analysed and the results reported (Ancelet and Davy 2016). However, a further year of sampling has been undertaken since then, which provided the opportunity to re-examine the PM_{10} dataset with the additional elemental speciation data and update the receptor modelling for PM_{10}. This has then formed the basis with which to compare the PM_{10} analysis with the $PM_{2.5}$ results.

PM_{10} samples in Richmond were collected using a Partisol sampler system, mainly on a 1-day-in-3 (midnight to midnight) sampling regime but switching to a 1-day-in-6 for the period September 2015 to October 2016. Overall, 313 samples were collected from June 2013 to October 2016. PM_{10} concentrations were determined gravimetrically and elemental and BC concentrations were determined using XRF and light reflection, respectively, as described in Appendix 1. Gravimetric results for the PM_{10} samples are presented in Figure 4.11. A clear seasonal pattern is apparent from Figure 4.11, with PM_{10} concentrations peaking from May–August. Outside of the winter season, PM_{10} concentrations were lower. Gaps present in Figure 4.11 resulted from missed sample days or samples removed as part of the quality assurance process, which could include, but would not be limited to, routine maintenance or equipment failure.

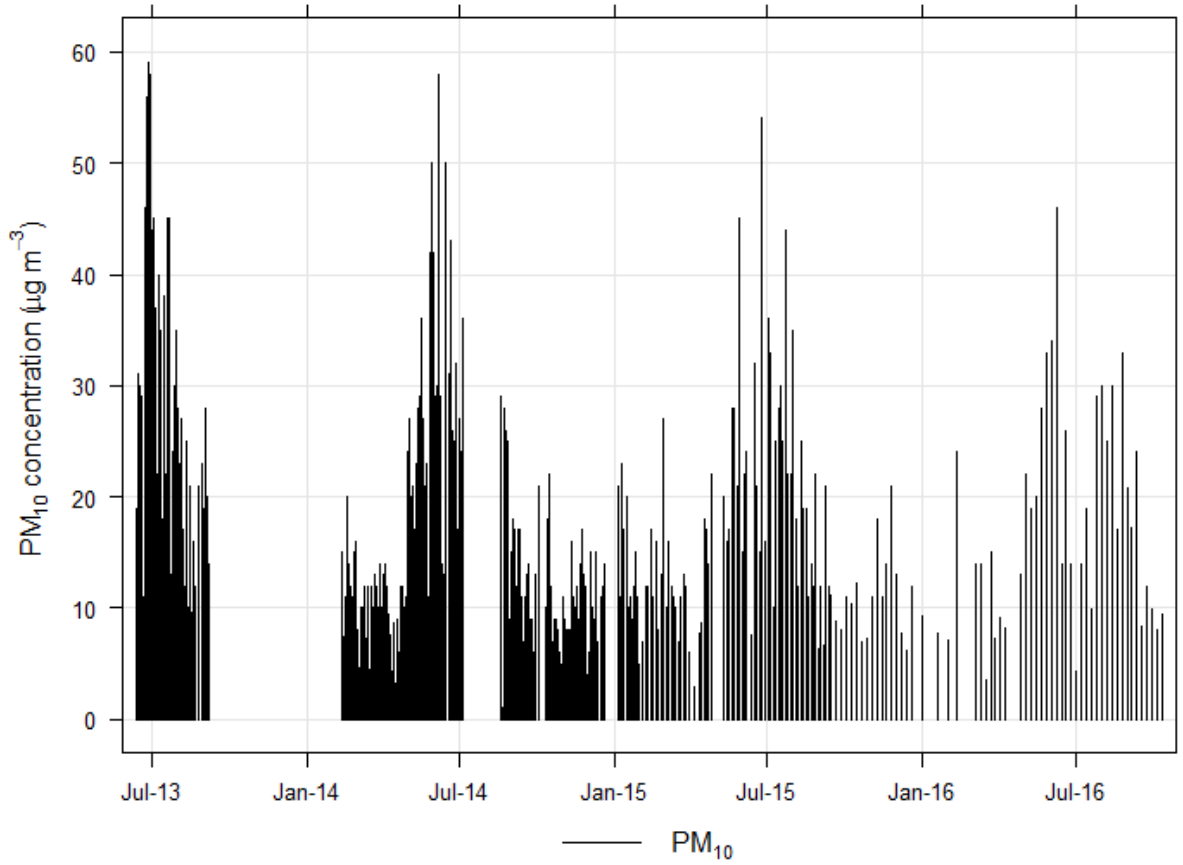

Figure 4.11 Gravimetric PM_{10} results from the Richmond monitoring site. Gaps are from missed sample days or samples removed as part of the quality assurance process.

4.2.1 Composition of PM_{10} at Richmond

Elemental concentrations in the PM_{10} samples collected are presented in Table 4.3 which shows that some measured species were close to or below their respective limit of detection (LOD) in each of the samples. Carbonaceous species, represented by BC, were found to dominate PM_{10} mass concentrations. Along with BC, other important elemental constituents included Na, Cl, Si, Al and S, indicating that combustion sources, marine aerosol, crustal matter and secondary sulphate particles are important contributors to PM_{10} concentrations at the monitoring site. An elemental correlation plot of PM_{10} components is provided in Appendix 2.

Table 4.3 Elemental concentrations in PM_{10} samples from Richmond (313 samples).

	Average (ng m^{-3})	Maximum (ng m^{-3})	Minimum (ng m^{-3})	Median (ng m^{-3})	Std Dev (ng m^{-3})	Uncertainty (ng m^{-3})	LOD (ng m^{-3})	% > LOD
PM_{10}	**17300**	**59000**	**1000**	**14000**	**11000**			
BC	3866	12665	297	2855	3245	379	162	100
Na	688	3519	5	509	592	179	141	88
Mg	165	509	0	163	88	20	5	97
Al	272	1086	10	220	187	45	26	98
Si	442	1773	0	361	338	61	25	98
P	2	24	0	0	5	15	20	1
S	257	645	30	247	121	40	21	100
Cl	999	7198	14	563	1137	104	6	100
K	276	975	42	215	185	31	5	100
Ca	173	619	4	150	106	21	6	100
Ti	16	65	0	13	12	6	5	83
V	1	8	0	0	1	3	4	6
Cr	14	215	0	1	35	3	2	42
Mn	5	17	0	5	4	3	2	66
Fe	189	665	11	155	126	21	2	100
Co	0	4	0	0	0	7	10	0
Ni	0	4	0	0	1	2	2	4
Cu	13	130	0	6	21	5	4	75
Zn	18	109	0	13	16	6	5	84
Ga	0	5	0	0	1	54	20	8
As	14	131	0	6	21	3	2	62
Se	0	7	0	0	1	21	31	0
Br	10	84	0	6	12	14	14	21
Sr	2	10	0	1	2	10	12	0
Y	0	4	0	0	1	12	17	0
Zr	1	11	0	0	2	18	25	0
Nb	2	11	0	1	2	16	21	0
Mo	2	10	0	2	2	21	28	0
Pd	2	23	0	0	3	11	14	0
Cd	2	16	0	1	3	14	17	0
Sn	4	21	0	2	4	17	20	0
Sb	4	32	0	2	5	16	19	2
Te	3	28	0	0	5	18	22	2
Cs	5	66	0	0	8	19	22	4
Ba	9	72	0	3	13	21	23	14
La	10	76	0	1	15	20	22	18
Ce	39	429	0	0	65	102	122	12
Sm	71	371	0	51	77	45	47	51
Pb	7	34	0	6	7	4	4	65

As for $PM_{2.5}$ (since $PM_{2.5}$ is a subset of PM_{10}), Table 4.3 shows that some of the heavy metal elements are present at significant concentrations above their respective LOD, particularly for arsenic and lead. The temporal variation for PM_{10} arsenic and lead as shown in Figure 4.12 also demonstrates a winter peak for both contaminants. Similar to $PM_{2.5}$, PM_{10} arsenic concentrations had significant non-winter peaks as found in the previous study (Ancelet and Davy 2016).

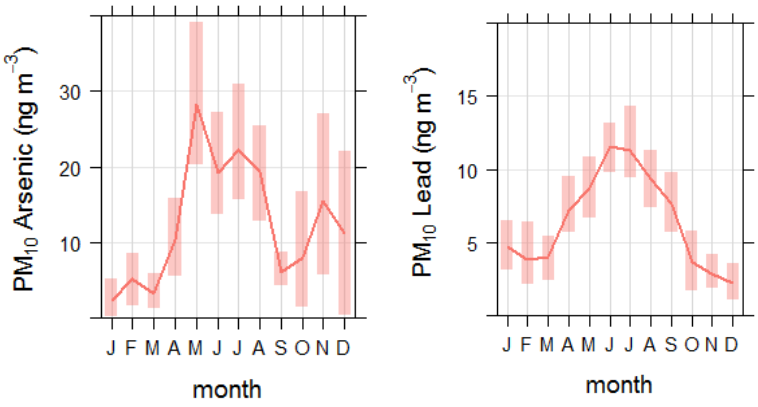

Figure 4.12 Temporal variation for PM_{10} arsenic (left); and lead (right) showing peak winter concentrations. Shaded areas represent the 95% confidence intervals.

The New Zealand ambient air quality guidelines (NZAAQG) provide guideline values for arsenic in PM_{10} (inorganic arsenic is 5.5 ng m^{-3} as an annual average) and lead (200 ng m^{-3} as a 3-month moving average, calculated monthly) in PM_{10} (MfE 2002). The calculation of an annual average for arsenic from the Richmond data was possible for 2014 and 2015 since these were the only years that monitoring covered the entire period (i.e. > 75 % coverage of the entire calendar year). For 2014 and 2015, the annual average arsenic concentrations in PM_{10} were 13 (±3) ng m^{-3}, and 16 (±3) ng m^{-3} respectively, significantly higher than the NZAAQG value. Table 4.3 indicates that the long-term average (2013 to 2016) for arsenic is of a similar value (14 ±3 ng m^{-3}). The 3-month moving average PM_{10} lead concentrations peaked during winter at around 10-12 ng m^{-3}, less than the NZAAQG of 200 ng m^{3}.

4.2.2 Source Contributions to PM_{10} in Richmond

Five source contributors were identified from PMF receptor modeling analysis of the PM_{10} data from Richmond. Table 4.4 and Figure 4.13 present the average elemental concentration source profiles extracted from the PMF analysis. The source contributors identified were found to explain 96% of the gravimetric PM_{10} mass on average.

The sources identified were:

- Biomass combustion: The first factor was identified as biomass combustion based on the dominance of BC and K in the profile (Fine, Cass et al. 2001, Khalil and Rasmussen 2003). Arsenic and Pb were strongly associated with the biomass combustion profile. This phenomenon is consistent throughout New Zealand and indicates that residents are burning copper chrome arsenate (CCA) treated and lead-painted timber, respectively (Ancelet et al. 2012);
- Motor vehicles: the second factor was identified as motor vehicles because of the presence of BC, Al, Si, Ca, Ti and Fe as significant elemental components. This profile is likely to be a combination of a motor vehicle tailpipe emissions (with BC representing fuel combustion) and re-entrained road dust emissions (Al, Si, Ca, Ti, and Fe as the crustal matter components);

- Secondary sulphate: the third factor was identified as secondary sulphate because of the dominance of S in the profile. This source contribution was likely to be associated with secondary sulphate aerosol produced in the atmosphere from gaseous precursors;
- Marine aerosol: the fourth factor was identified as a marine aerosol source because of the predominance of Na and Cl, along with some Mg, S, K, and Ca;
- CCA: the fifth factor was identified as originating from emissions of copper chrome arsenate (CCA) containing particulate matter. This is a similar result as identified for $PM_{2.5}$ and in the previous PM_{10} (June 2013 – September 2015) analysis.

Table 4.4 Source elemental concentration profiles for PM_{10} samples from Richmond.

	Biomass combustion (ng m^{-3})	Motor vehicles (ng m^{-3})	Secondary sulphate (ng m^{-3})	Marine aerosol (ng m^{-3})	CCA (ng m^{-3})
PM_{10}	8500	3700	2300	2600	140
BC	3299.7	590.7	0.0	53.3	4.6
Na	13.5	70.1	118.9	474.8	12.4
Mg	9.9	19.7	41.2	77.5	7.7
Al	5.9	199.7	36.2	24.1	1.6
Si	6.2	352.5	60.3	13.4	0.9
S	28.3	42.3	89.2	89.1	3.3
Cl	38.3	50.3	32.7	843.7	18.8
K	149.7	50.6	34.4	26.2	5.2
Ca	7.6	110.2	22.2	24.3	3.8
Ti	0.6	11.6	2.1	0.5	0.3
Cr	0.0	0.8	0.0	0.4	12.1
Mn	0.6	2.7	0.9	0.0	0.3
Fe	24.6	129.3	24.5	9.3	0.2
Cu	1.9	1.9	0.2	1.1	7.0
Zn	11.5	4.2	0.4	0.5	0.1
As	5.8	0.0	0.3	0.0	6.7
Pb	4.0	0.0	1.1	0.5	0.0

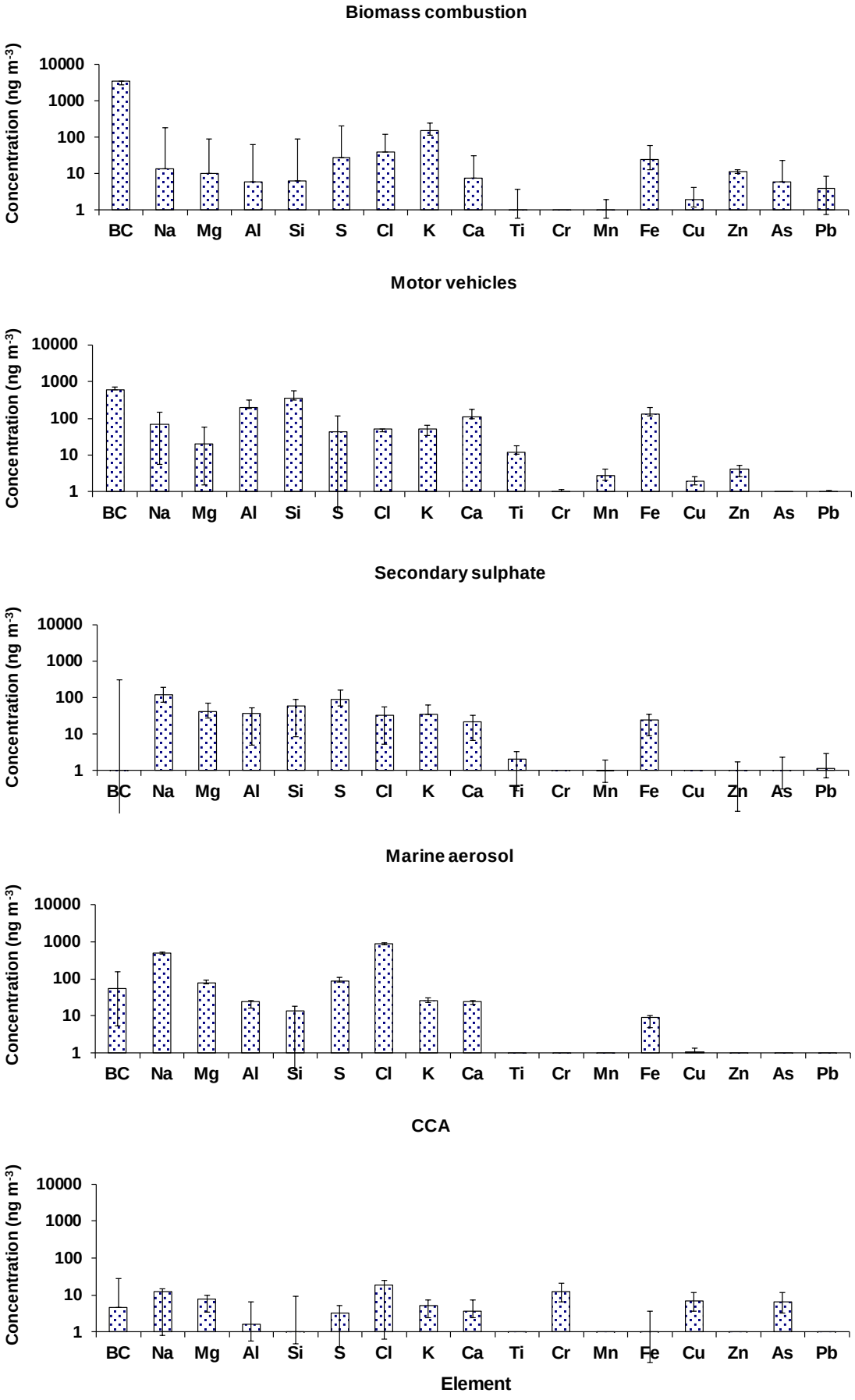

Figure 4.13 Source elemental concentration profiles for PM_{10} samples from Richmond.

Figure 4.14 presents the relative source contributions to PM_{10} in Richmond. Also included in Figure 4.14 are the 5th and 95th percentile confidence limits in PM_{10} mass attributed to each of the sources.

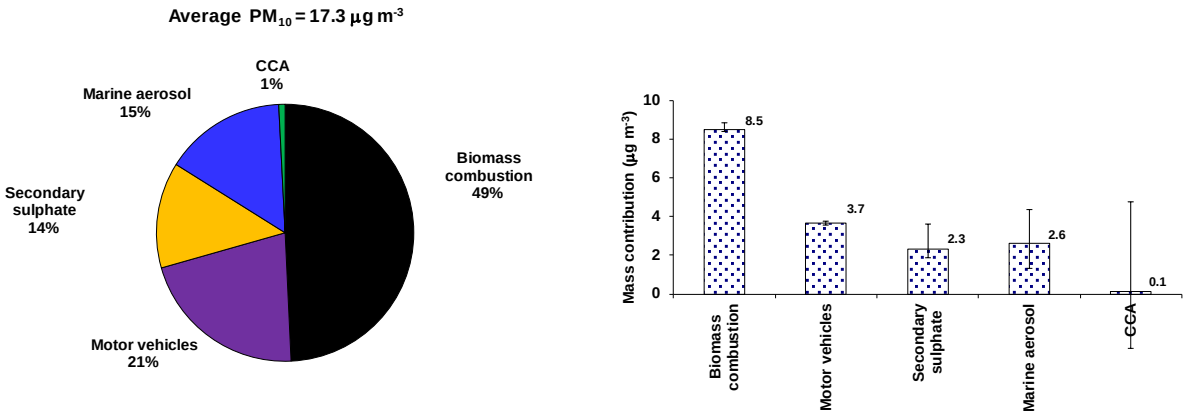

Figure 4.14 Average source contributions to PM_{10} in Richmond over the monitoring period (June 2013 – October 2016).

The average PM_{10} source contributions over the entire monitoring period estimated from the PMF analysis showed that biomass combustion was the most significant contributor to PM_{10} mass (49%). motor vehicles (21%), secondary sulphate (14%), marine aerosol (15%) and had lesser contributions to PM_{10} mass, while CCA had the lowest (trace) contribution (1%).

Temporal variations in the source contributions are presented in Figure 4.15 (note the difference in concentration scales and that gaps in the data are due to missing sample periods). It was evident that PM mass is dominated by the biomass combustion source during winter, which arises primarily from emissions from solid fuel fires used for domestic heating. During other time periods, marine aerosol, sulphate and motor vehicle contributions were the primary sources contributing to PM_{10}. The PM due to the CCA source was present intermittently at relatively low concentrations.

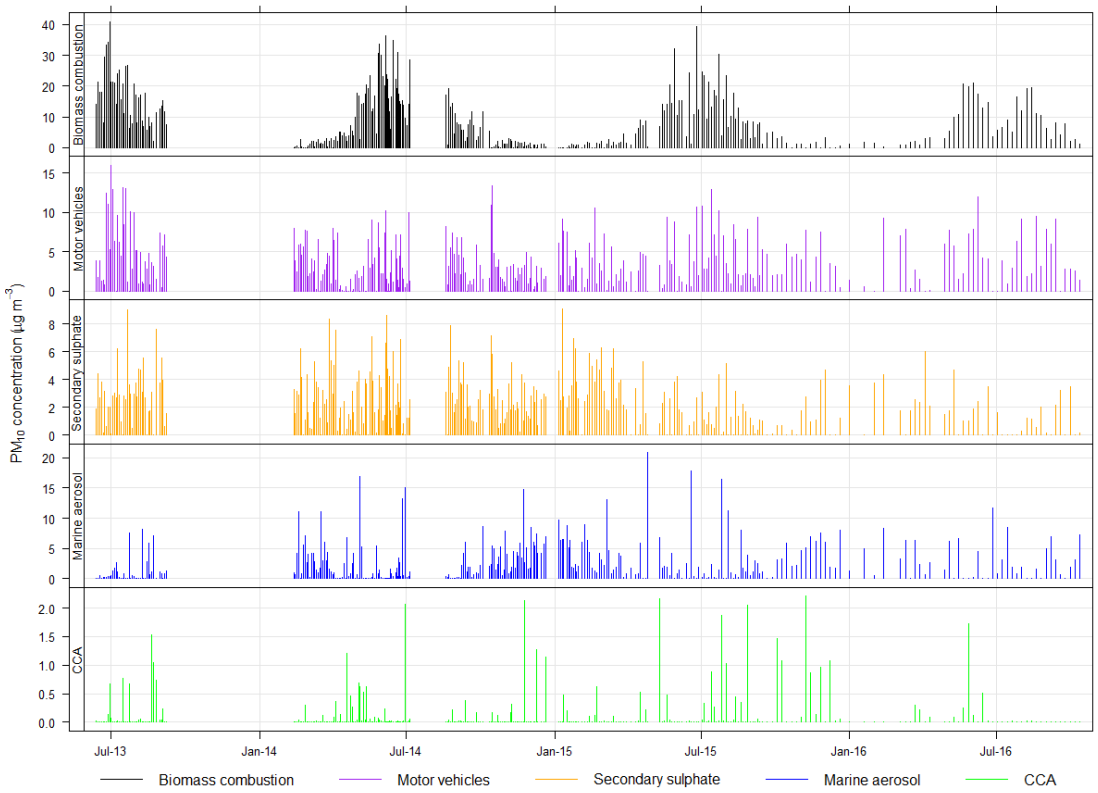

Figure 4.15 Temporal variations in relative source contributions to PM_{10} mass. Note the difference in each of the numerical scales.

4.2.3 Seasonal Variations in PM_{10} Sources at Richmond

PM_{10} was found to peak in Richmond from late Autumn until the end of winter (May to September). Figure 4.16 and Figure 4.17 present average monthly PM_{10} concentrations and source contributions, respectively. The dominant source of PM_{10} from May to September in Richmond was biomass combustion associated with solid fuel fire emissions for domestic heating and was clearly the driver of PM_{10} concentrations over the winter period. Some seasonality was apparent in the marine aerosol and sources, which peaked during spring and summer when wind speeds tend to increase. Some seasonality in concentrations was observed for the secondary sulphate source with peak summer concentrations in line with solar forcing of atmospheric chemistry coupled with source activity. Otherwise, little seasonality was apparent in the motor vehicle and CCA sources.

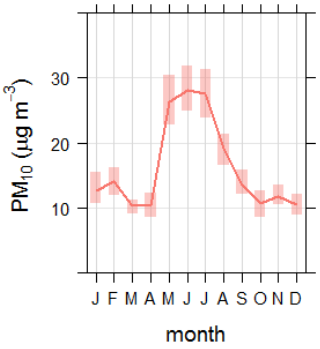

Figure 4.16 Average monthly PM_{10} concentrations in Richmond. Shaded areas represent the 95% confidence intervals.

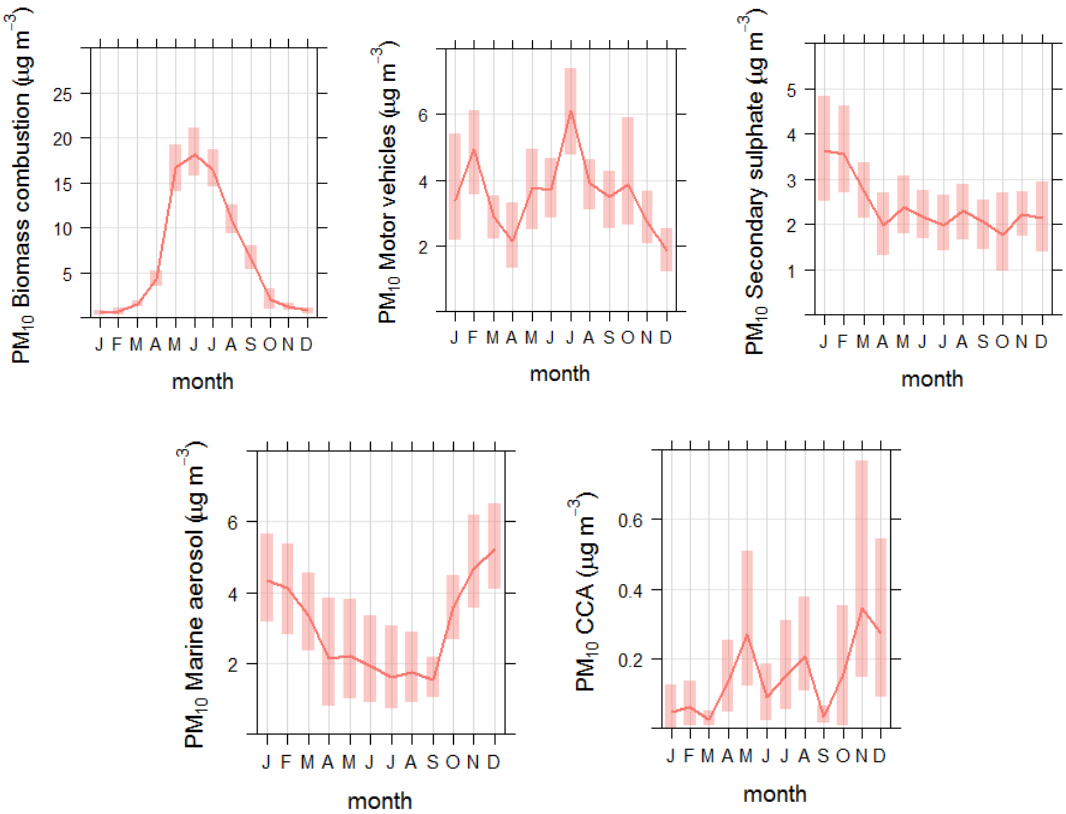

Figure 4.17 Average monthly source contributions to PM_{10} in Richmond. Shaded areas represent the 95% confidence intervals.

4.2.4 Daily Variations in PM_{10} Sources at Richmond

Source contributions to PM_{10} concentrations were analysed by day of the week to investigate any potential weekday/weekend variations. Figure 4.18 presents PM_{10} concentration variations by day of the week. It was evident that PM_{10} concentrations were not statistically different day-to-day, and no weekday/weekend difference was apparent. However, as for $PM_{2.5}$ analysis of source contributions revealed that the motor vehicle source contributions were significantly lower on weekends than weekdays (Figure 4.19), and is likely to be indicative of lower traffic densities during the weekend than weekdays associated with normal working week and commuter behaviour.

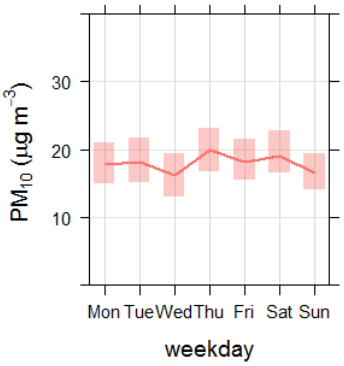

Figure 4.18 Variation in PM_{10} concentrations in Richmond by day of the week. Shaded areas represent the 95% confidence intervals.

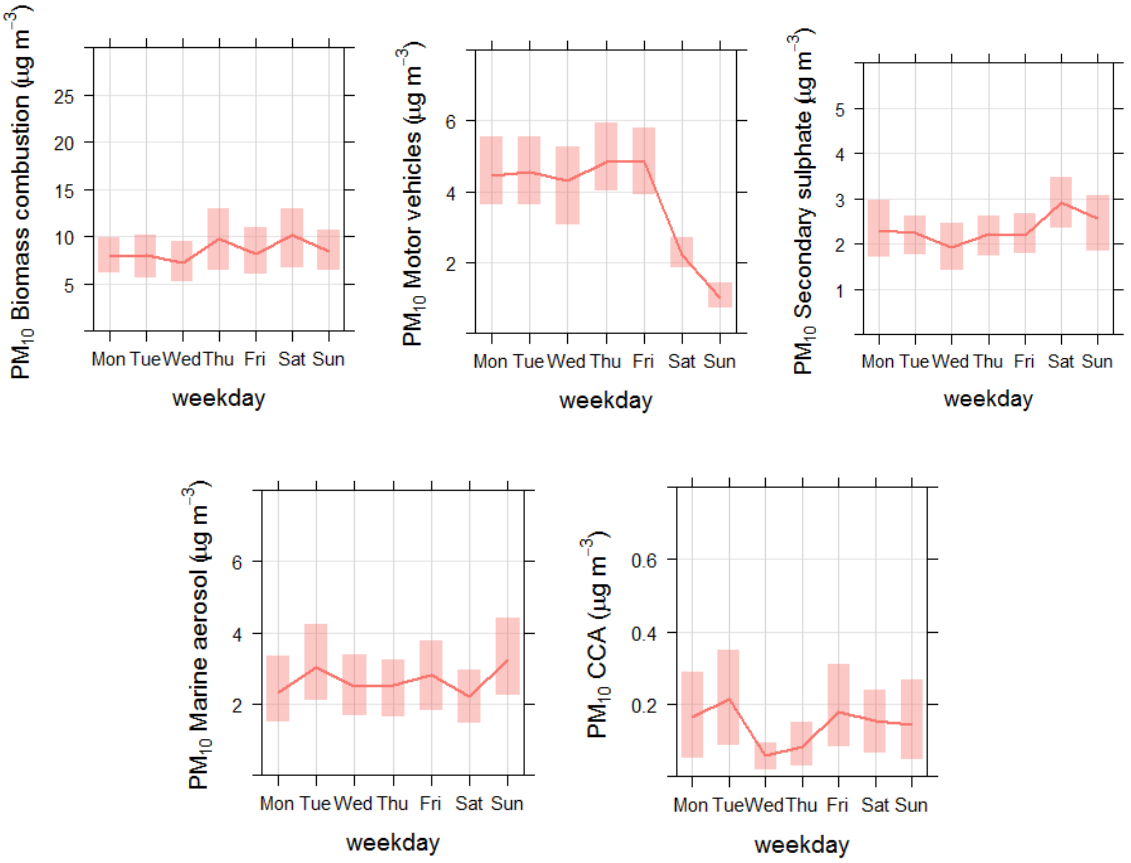

Figure 4.19 Variation in source contributions to PM_{10} in Richmond by day of the week. Shaded areas represent the 95% confidence intervals.

4.3 Variations in $PM_{2.5}$ and PM_{10} Source Contributions in Richmond with Wind Direction

It is evident from the data that similar sources contribute to both $PM_{2.5}$ and PM_{10}, therefore the dominant direction from which the sources arrive at the Richmond monitoring station should also be similar. However, it should be kept in mind that the $PM_{2.5}$ monitoring was for one year, whereas the PM_{10} monitoring spans three years and there is the potential for interannual differences. This can be seen in the windspeed and direction data underlying the $PM_{2.5}$ and PM_{10} bivariate polar plots presented in the following sections. Bivariate polar plots using the source contributions to $PM_{2.5}$ and PM_{10} were produced using R statistical software and the openair package (Team 2011, Carslaw 2012, Carslaw and Ropkins 2012). Using bivariate polar plots, source contributions can be shown as a function of both wind speed and direction, providing invaluable information about potential source regions and how pollution from a specific source builds up. To produce the polar plots, wind speeds and directions were vector averaged using functions available in openair. A full description of the vector averaging process can be found in Carslaw (2012). The statistic = "weighted.mean" has been used here because it provides an indication of the concentration × frequency of occurrence and will highlight the wind speed/direction conditions that dominate the overall mean contribution of the source. Because of the smoothing involved, the colour scale is only to provide an indication of overall pattern and should not be interpreted in concentration units e.g. for statistic = "weighted.mean", where the bin mean is multiplied by the bin frequency and divided by the total frequency. Note that the meteorological data used for the polar plot analysis was that supplied by TDC from their Queen Street site.

4.3.1 Biomass Combustion

Biomass combustion source contributions to $PM_{2.5}$ and PM_{10} are considered to be primarily from domestic solid fuel fire emissions. Figure 4.20 presents a bivariate polar plot of biomass combustion contributions showing that peak biomass combustion contributions to both $PM_{2.5}$ and PM_{10} occurred under low wind speeds from the southwest. This indicates that katabatic flows under cold and calm anticyclonic synoptic meteorological conditions coupled with domestic fire emissions and poor dispersion were likely responsible for elevated particle concentrations, similar to previous results in other New Zealand locations (Ancelet, Davy et al. 2012, Ancelet, Davy et al. 2013). Such meteorological conditions can reasonably be anticipated one or two days ahead of time so that it can be used as a predictor of high concentrations of particulate matter pollution due to domestic fires or to issue warnings of an air pollution risk.

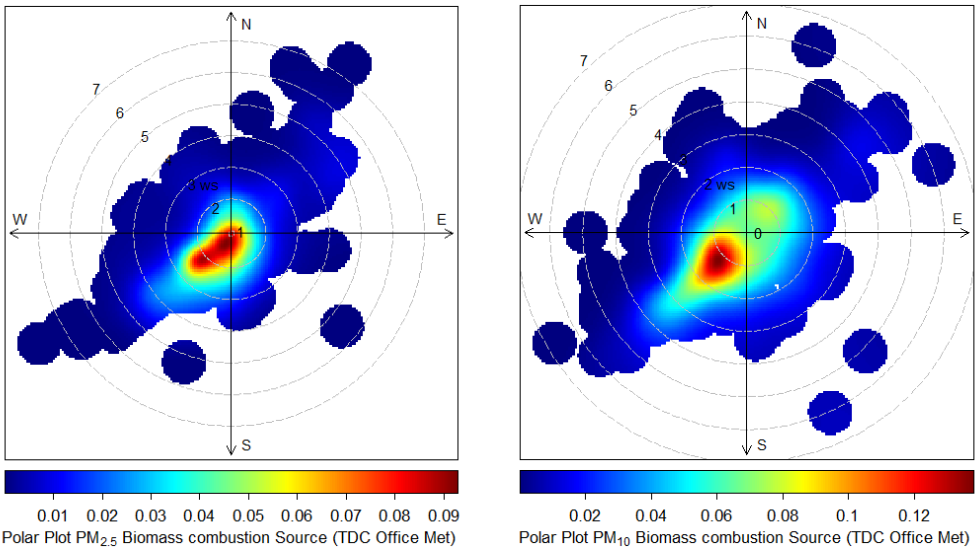

Figure 4.20 Polar plot of biomass combustion contributions to $PM_{2.5}$ (left) and PM_{10} (right) concentrations. The radial dimensions indicate the wind speed in 1 m s^{-1} increments and the colour contours indicate the average contribution to each wind direction/speed bin.

4.3.2 Motor Vehicles

The greatest $PM_{2.5}$ motor vehicle contributions (i.e. largely tailpipe emissions) at the monitoring site occurred under winds from the north, while PM_{10} motor vehicle contributions (which have a significant road dust component) were influenced by winds from the north and southwest (Figure 4.21). This supports the assignment of the motor vehicle source (including road dust) since SH6, the main arterial route between Richmond and Nelson, is located in this sector (running southwest to northeast) relative to the monitoring site with the major component of the road (acting as a line source) to the north.

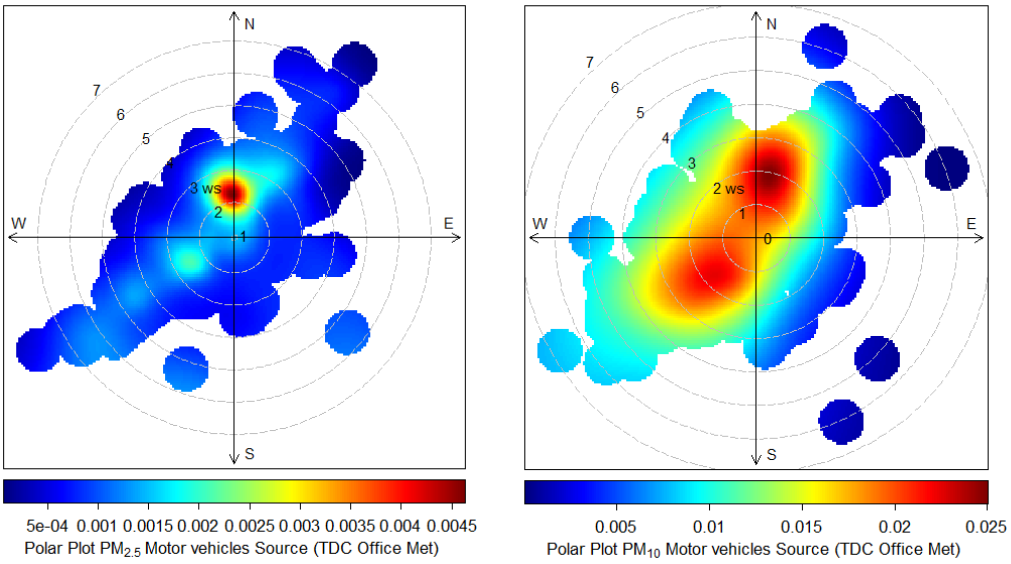

Figure 4.21 Polar plot of motor vehicle contributions to $PM_{2.5}$ (left) and PM_{10} (right) concentrations. The radial dimensions indicate the wind speed in 1 m s^{-1} increments and the colour contours indicate the average contribution to each wind direction/speed bin.

4.3.3 Secondary Sulphate

Secondary sulphate contributions to both $PM_{2.5}$ and PM_{10} in Richmond originated from north of the monitoring site (Figure 4.22). It is possible that shipping emissions from the Nelson Port contributed to the secondary sulphate concentrations. However, other sources of secondary sulphate include natural emissions (marine phytoplankton and volcanic sources) and industrial emissions. Further discussion on the secondary sulphate source is provided in Section 5.1.3.

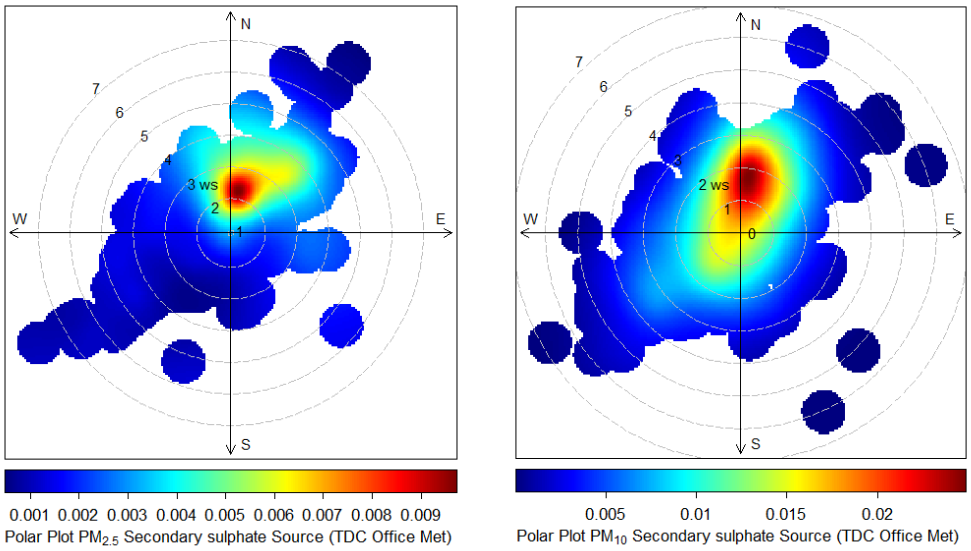

Figure 4.22 Polar plot of secondary sulphate contributions to $PM_{2.5}$ (left) and PM_{10} (right) concentrations. The radial dimensions indicate the wind speed in 1 m s^{-1} increments and the colour contours indicate the average contribution to each wind direction/speed bin.

4.3.4 Marine Aerosol

Marine aerosol contributions in Richmond peaked under high wind speeds primarily from the northeast (Figure 4.23). The most likely sources of marine aerosol were the Tasman Sea and Southern Ocean.

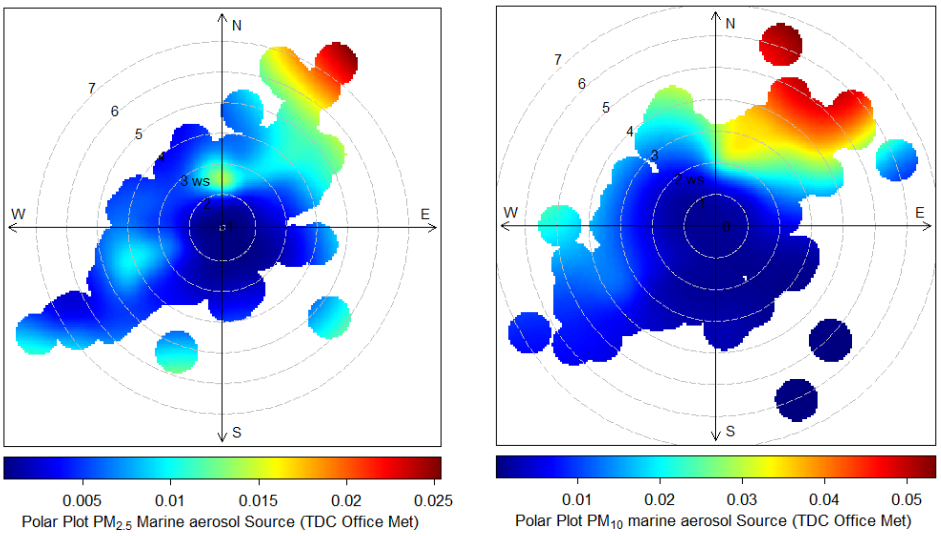

Figure 4.23 Polar plot of marine aerosol contributions to $PM_{2.5}$ (left) and PM_{10} (right) concentrations. The radial dimensions indicate the wind speed in 1 m s^{-1} increments and the colour contours indicate the average contribution to each wind direction/speed bin.

4.3.5 CCA

Figure 4.24 shows that the CCA source contributions peaked under moderate to high wind speeds from the northeast. In an earlier analysis[2] that examined the influence of wind speed and direction on the individual primary elemental components (copper, chromium and arsenic) of the CCA source for both $PM_{2.5}$ and PM_{10}, it was shown that they too demonstrated a similar source directionality. It is reasonably clear from the polar plots presented in Figure 4.24 that, that the CCA source contributions to both PM_{10} and $PM_{2.5}$, moderate north-northeast wind conditions dominate the overall mean concentrations indicating that the potential emission source is likely to be north-northeast of the Richmond air quality monitoring site.

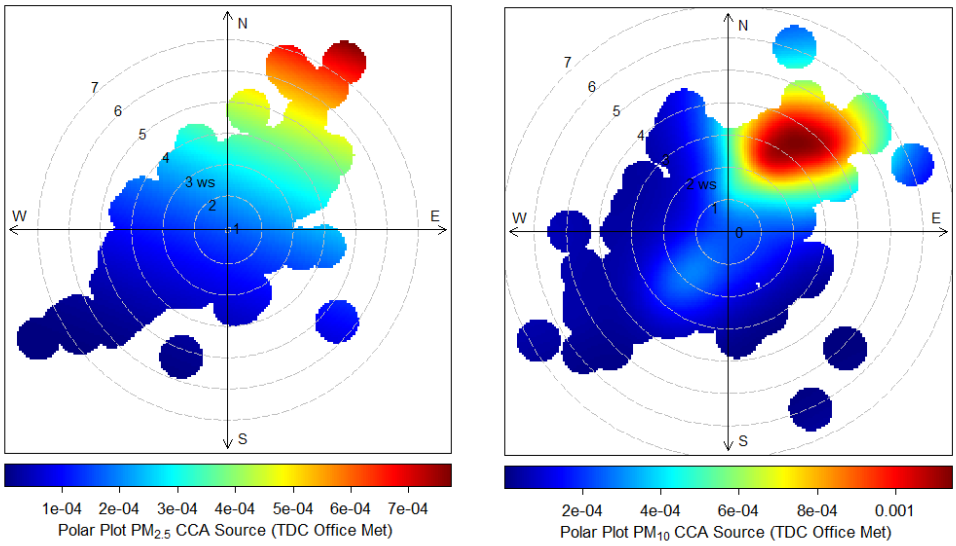

Figure 4.24 Polar plot of CCA contributions to $PM_{2.5}$ (left) and PM_{10} (right) concentrations. The radial dimensions indicate the wind speed in 1 m s^{-1} increments and the colour contours indicate the average contribution to each wind direction/speed bin.

[2] *Davy, P.K., Elemental arsenic, copper and chromium concentrations at Richmond, GNS Science Letter Report CR 2017/03 LR*

5.0 DISCUSSION OF THE RECEPTOR MODELING RESULTS

Monitoring of $PM_{2.5}$ and PM_{10} in Richmond shows that concentrations peak during the winter and that the NESAQ for PM_{10} was exceeded on several occasions. Five source contributors to both $PM_{2.5}$ and PM_{10} were identified from the receptor modeling analyses. The receptor modeling analysis showed that some source contributors had distinct seasonalities and that particulate matter concentrations were primarily influenced by local emission sources.

5.1 COMPARISON OF $PM_{2.5}$ AND PM_{10} CONCENTRATIONS AND SOURCES IN RICHMOND

This section presents a comparison between the results from the receptor modelling analyses of the $PM_{2.5}$ and PM_{10} datasets from the Richmond site (October 2015 – October 2016). The two sample sets were independently collected and therefore serve as a crosscheck on the veracity of the receptor modelling analysis as well as providing the opportunity to assess the relative contribution of coarse particle mass from each source. Note that only the coincident $PM_{2.5}$ and PM_{10} samples collected at Richmond have been considered here since $PM_{2.5}$ sampling was daily but PM_{10} was sampled on a 1-day-in-6 monitoring regime. There were a total of 54 coincident PM_{10} and $PM_{2.5}$ samples over the monitoring period. Table 5.1 lists the average source contributions determined for each of the sample sets and Figure 5.1 presents the corresponding pie graphs which are essentially the same as for the contributions over the entire $PM_{2.5}$ and PM_{10} datasets respectively.

Table 5.1 Average source mass contributions (± modelled standard deviation) derived for the two Richmond particulate matter size fraction datasets.

Source	Biomass burning ($\mu g\ m^{-3}$)	Motor vehicles ($\mu g\ m^{-3}$)	Secondary sulphate ($\mu g\ m^{-3}$)	Marine aerosol ($\mu g\ m^{-3}$)	CCA ($\mu g\ m^{-3}$)
$PM_{2.5}$	8.2±0.9	0.3±0.3	0.8±0.5	1.0±0.3	0.04±0.1
PM_{10}	6.0±1.9	3.9±0.6	1.5 ±0.8	3.3±0.2	0.2±0.1

Immediately evident from Table 5.1 and Figure 5.1 is the dominance of biomass combustion sources over $PM_{2.5}$ concentrations and the higher mass contribution to PM_{10} (compared to $PM_{2.5}$) from marine aerosol and motor vehicle sources due to the coarse particle ($PM_{10\text{-}2.5}$) content generated by these sources. The biomass burning is primarily a $PM_{2.5}$ source with a similar $PM_{2.5}$ and PM_{10} mass (within the bounds of uncertainty). Secondary sulphate is also a fine particle source but some of the sulphate particle size range does extend into the coarse fraction (Anlauf, Li et al. 2006), particularly where heterogeneous atmospheric chemistry takes place on the surface of particles (such as for shipping emissions) or in aerosol droplets during the reaction of sulphur gaseous species to form secondary sulphate particle species (Gard, Kleeman et al. 1998, O'Dowd, Lowe et al. 2000, George and Abbatt 2010).

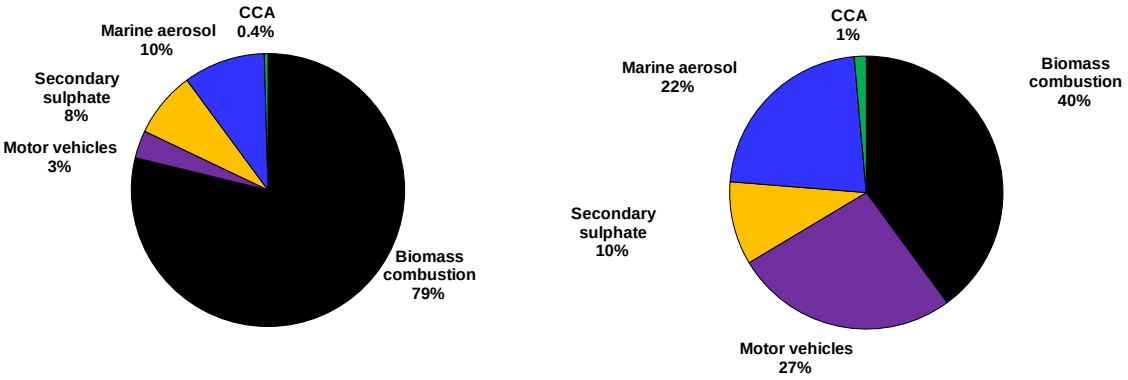

Figure 5.1 Average source contributions for coincident monitoring results (left) $PM_{2.5}$ and; (right) PM_{10} results

The motor vehicle source has higher mass contributions to PM_{10} than $PM_{2.5}$ and this is due to a coarse particle road dust component covariant with tailpipe emissions. The PM_{10} source profile for the motor vehicle sources shows this with a much higher crustal matter component (Al, Si, Ca, Ti, Fe) than the corresponding $PM_{2.5}$ motor vehicle source profiles (see Table 4.2 and Table 4.4 for the $PM_{2.5}$ and PM_{10} source profiles respectively). Figure 5.2 illustrates the relationship between the $PM_{2.5}$ and PM_{10} sources showing that they were highly correlated between the two sample sets with variation around the relative importance of coarse particle mass contribution from each source. Figure 5.2 also shows that the biomass combustion source dominates $PM_{2.5}$ and PM_{10} mass concentrations.

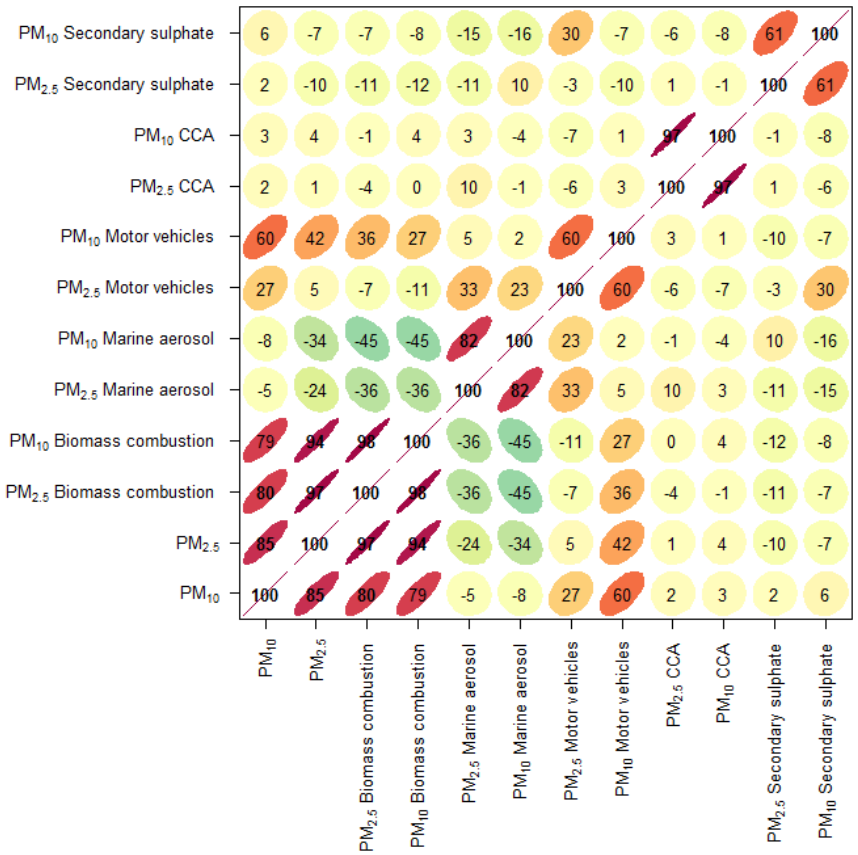

Figure 5.2 Correlation plot for $PM_{2.5}$ and PM_{10} mass concentration and source contribution results.

5.2 DISCUSSION OF $PM_{2.5}$ AND PM_{10} SOURCES IN RICHMOND

5.2.1 Biomass Combustion

Analysis of temporal and seasonal trends showed that $PM_{2.5}$ and PM_{10} from biomass combustion peaked during the winter and showed no variation between days of the week. The lack of variation between days of the week was not surprising because peak biomass combustion contributions occur under meteorological conditions conducive to the build-up of pollutants (cold, calm, anticyclonic conditions). The biomass combustion source originates from domestic wood combustion for home heating and also includes arsenic and lead in the profile, suggesting that CCA-treated and lead-painted wood is being included as fuel. It was found that the annual average arsenic concentrations in PM_{10} for 2014 (13 ng m^{-3}) and 2015 (16 ng m^{-3}) exceeded the NZAAQG (5.5 ng m^{-3} as an annual average). As found in the previous analyses, this study has shown that there were two sources of arsenic containing particulate matter. The data behind Table 4.2 and Table 4.4 show that the biomass combustion source contributed 4 ng m^{-3} arsenic on average to both $PM_{2.5}$ and PM_{10} over the same monitoring period (September 2015 – October 2016) indicating that the arsenic associated with biomass combustion was all in the $PM_{2.5}$ fraction. Arsenic concentrations from biomass combustion (in PM_{10}) were calculated to be 5.2 ng m^{-3} and 4.7 ng m^{-3} as annual averages for 2014 and 2015 respectively. The use of such contaminated timber as fuel for domestic fires appears to be common throughout New Zealand including Nelson (Davy, Trompetter et al. 2010, Davy, Trompetter et al. 2011, Ancelet, Davy et al. 2012, Davy, Ancelet et al. 2012, Davy and Ancelet 2014, Davy, Ancelet et al. 2014).

Biomass combustion was identified to be responsible for peak $PM_{2.5}$ and PM_{10} concentrations, and for consequent exceedances of the NES. Further discussion on peak events is provided in Section 5.3.

5.2.2 Motor Vehicles

The motor vehicle source identified is a combination of vehicular tailpipe emissions (and re-suspended soil generated by the turbulent passage of vehicles on roads, carparking areas and unsealed yards. Often in urban areas, re-entrained crustal matter on roads (i.e. road dust) is the primary source of the soil component. Further support for the anthropogenic origin of this source is that weekday contributions were significantly higher than for weekends indicating an association with traffic density in line with commuter and commercial vehicle behaviour. The bivariate polar plots (Figure 4.21) depicting the variation of the source contributions with wind speed and direction showed that peak concentrations occurred under winds from the north southwest, coinciding with the location of SH6 (as a line source), the major local arterial roadway which runs between Richmond and Nelson.

5.2.3 Secondary Sulphate

The $PM_{2.5}$ and PM_{10} secondary sulphate source showed higher concentrations during summer months though with some variability around this. Analysis of the sulphate source contributions variation with wind speed and direction using polar plots showed that sulphate was transported from north of the sampling site. Sources of secondary sulphate include emissions of sulphur dioxide precursor gas from shipping activities in the Nelson Port area (Davy, Trompetter et al. 2011, Ancelet, Davy et al. 2014). Longer range sources include marine phytoplankton activity (release of dimethyl sulphide as a gaseous precursor to secondary sulphate) and potentially emissions of SO_2 gas from the Central Plateau volcanic zone (Davy, Trompetter et al. 2009). The average secondary sulphate source contribution (2.3 µg m^{-3}) to PM_{10} in Richmond was

higher than for Wellington (1.2 µg m^{-3} at both Seaview and Wainuiomata) and for six Auckland sites (1.3–1.5 µg m^{-3}) Additionally, temporal variations in secondary sulphate concentrations normally demonstrate higher concentrations during summer (Davy, Trompetter et al. 2011, Davy, Ancelet et al. 2012) due the influence of solar forcing and cycles in natural source production. The Richmond data does not show such strong seasonality also indicating that there may be some localised emission source (such as shipping emissions) of precursor sulphur containing gases.

5.2.4 Marine Aerosol

The elemental composition for the marine aerosol source closely resembled that of seawater and the source profile is dominated by chlorine and sodium, as presented in source elemental profiles. Analysis of temporal and seasonal variations in marine aerosol showed higher concentrations during spring and summer, indicating that the generation of marine aerosol is dependent on meteorological factors, such as wind and evaporation potential. Analysis of marine aerosol contributions to PM_{10} concentrations showed distinct northeasterly directionality. Interestingly the average marine aerosol contribution to PM_{10} (2.6 µg m^{-3}) was lower than those found for Wainuiomata (5.9 µg m^{-3}) and Seaview (6.3 µg m^{-3}) in Wellington (Davy, Trompetter et al. 2008, Davy, Trompetter et al. 2009) and at six Auckland sites (6–7 µg m^{-3}) (Davy, Trompetter et al. 2009). The lower marine aerosol concentrations in Richmond may reflect a sheltering effect of the surrounding mountain ranges and somewhat calmer local meteorological conditions.

5.2.5 CCA

As found in the previous analyses, the CCA source was intermittent, showed no seasonality or weekday/weekend differences and was a minor contributor to overall $PM_{2.5}$ and PM_{10} concentrations but was a significant contributor to average arsenic concentrations. The CCA source dominated copper and chromium concentrations in both $PM_{2.5}$ and PM_{10}. Polar plots for the CCA source and elemental copper and chromium indicates that contributions increased under high wind speeds from the northeast, consistent with a point source emission in that direction (i.e. only detected at the site when source activity, wind conditions and particulate matter sampling coincided). The other clear distinction between the biomass combustion and CCA sources of arsenic was the association of copper and chromium with the CCA source which was likely to be due to the differing particulate source emission characteristics. Interestingly, when the concentrations of arsenic, copper and chromium associated with the CCA source were examined for coincident $PM_{2.5}$ and PM_{10} sampling days, it was found that the ratio of copper and chromium in PM_{10} compared to $PM_{2.5}$ was about 4:1, whereas the ratio for arsenic was about 2:1 as presented in Figure 5.3. All elements were highly correlated (R^2 = 0.95) between $PM_{2.5}$ and PM_{10}.

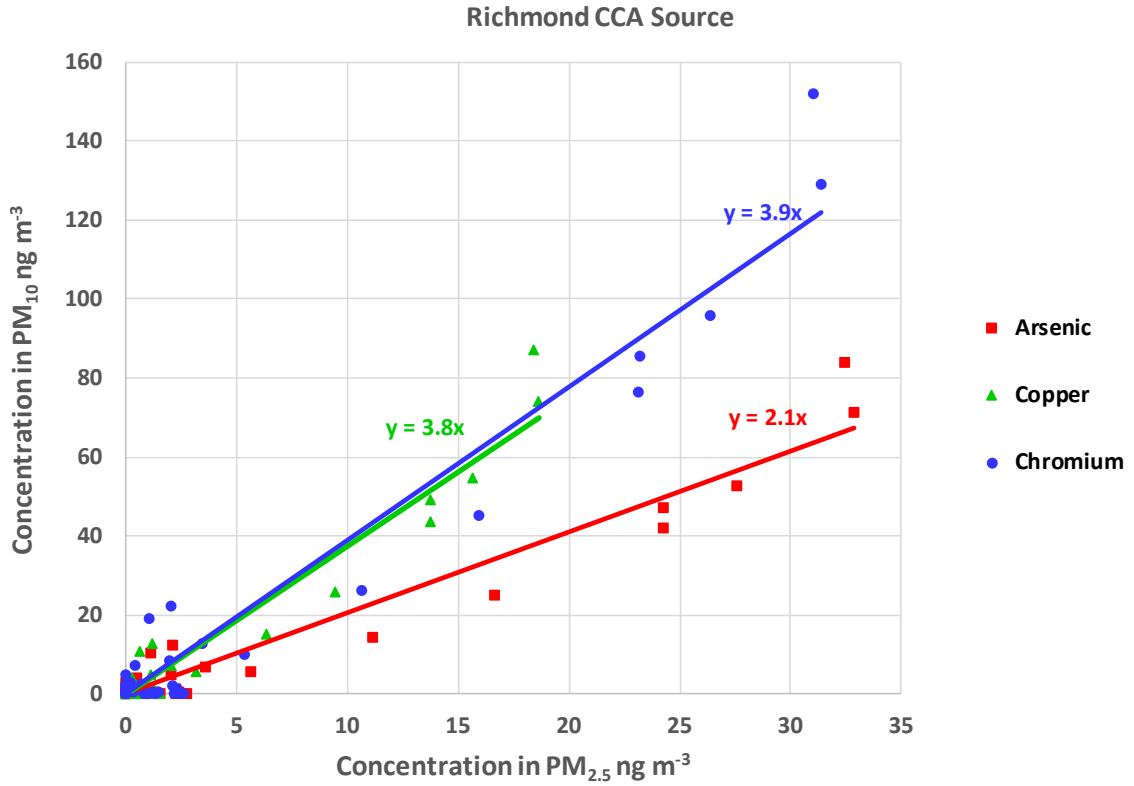

Figure 5.3 Plot of arsenic, copper and chromium concentrations attributed to the CCA $PM_{2.5}$ and PM_{10} sources in Richmond.

A study on the combustion of CCA treated timber suggests both +3 and +4 arsenic oxide states are released and some arsenic is retained in the ash (Helsen and van den Bulck 2003). It was also shown that the copper and chrome components are preferentially retained in the ash during combustion of CCA treated timber. The dichotomy observed in Figure 5.3 between As, Cu and Cr concentrations in $PM_{2.5}$ and PM_{10} suggests that there may be combustion particle ($<PM_{2.5}$) and fly ash ($PM_{10\text{-}2.5}$) components to the CCA source emissions. The data indicates that the CCA source contributed 7.5 ng m^{-3} arsenic on average to $PM_{2.5}$ and 10.4 ng m^{-3} to PM_{10} arsenic concentrations over the same monitoring period (September 2015 – October 2016). Arsenic concentrations from the CCA source (in PM_{10}) were calculated to be 5.3 ng m^{-3} and 7.5 ng m^{-3} as annual averages for 2014 and 2015 respectively.

5.3 ANALYSIS OF CONTRIBUTIONS TO PM_{10} ON PEAK DAYS

For air quality management purposes, understanding the contributions from the various sources to peak particulate matter pollution events are of most interest. Therefore, the mass contributions of sources to all PM_{10} concentrations over 33 µg m^{-3} and $PM_{2.5}$ concentrations over 17 µg m^{-3} (the Ministry for the Environment 'Alert' level as discussed in Section 2.1) are presented in Figure 5.4 and Figure 5.5 respectively.

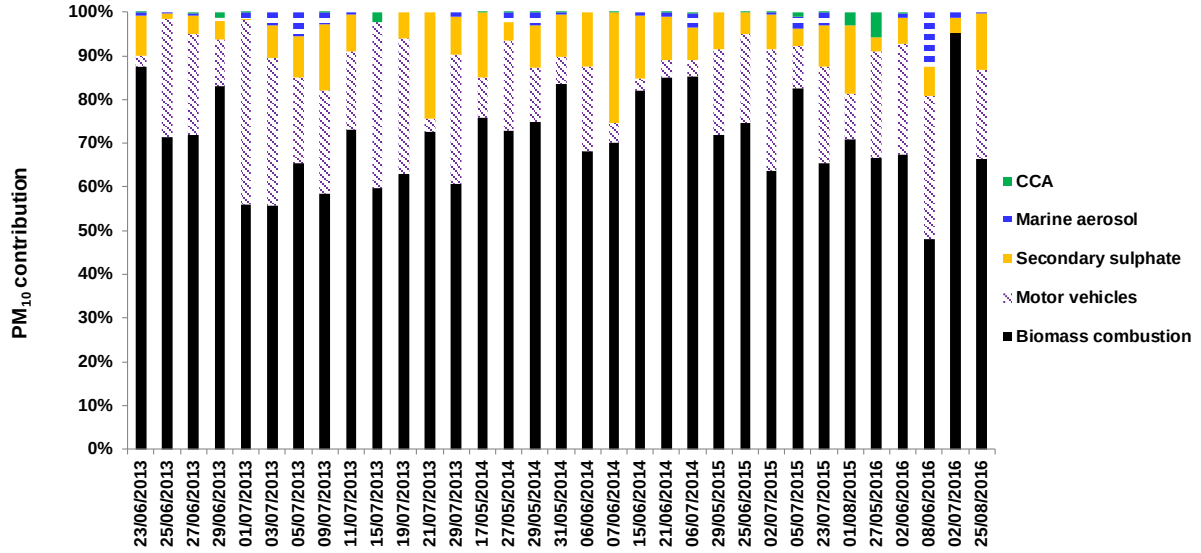

Figure 5.4 Mass contributions to peak PM_{10} events (> 33 µg m^{-3}) in Richmond.

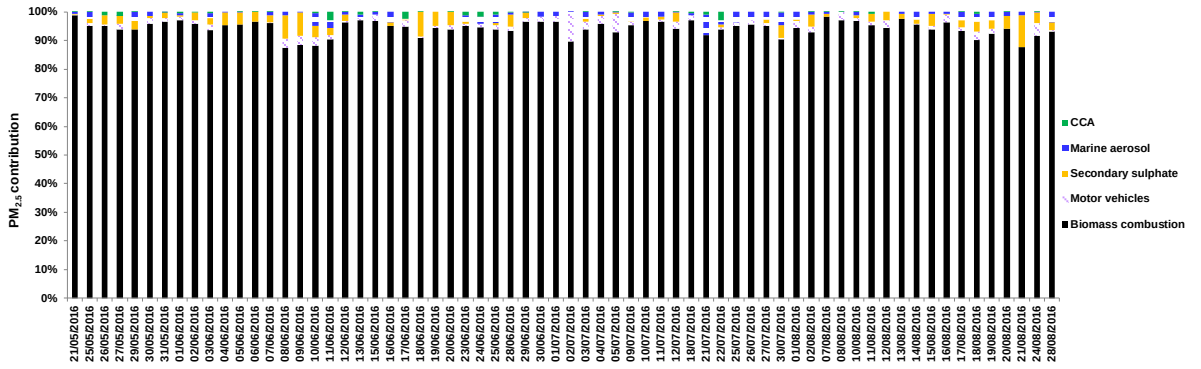

Figure 5.5 Mass contributions to peak $PM_{2.5}$ events (> 17 µg m^{-3}) in Richmond.

Figure 5.4 shows that peak PM_{10} events occurred primarily during winter, and that biomass combustion was responsible for an average of 70 % of PM_{10} mass on high pollution days. Furthermore, as found in other New Zealand urban areas (Davy, Ancelet et al. 2012, Ancelet, Davy et al. 2013, Ancelet, Davy et al. 2014), on high pollution nights during winter $PM_{2.5}$ in Richmond was dominated by biomass burning emissions (95 %) most of the particulate matter is in the fine fraction ($PM_{2.5}$). Figure 5.5 shows that there were many more days where $PM_{2.5}$ was in the 'alert' category and that fine particles from biomass combustion sources dominated concentrations.

Of the days during the monitoring period where PM_{10} exceeded the NESAQ (50 µg m^{-3}) in Richmond, biomass combustion was responsible for over 75 % of PM_{10} concentrations on average as shown in Figure 5.6.

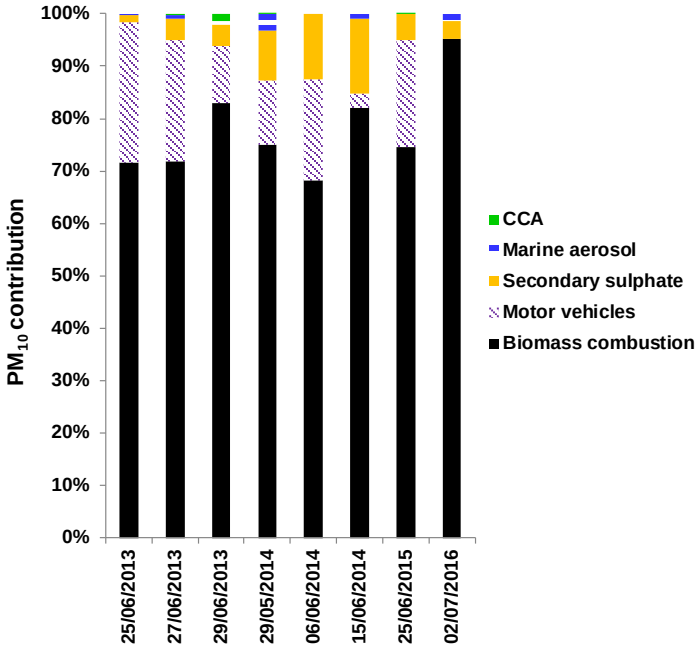

Figure 5.6 Mass contributions to PM_{10} exceedance events (> 50 µg m^{-3}) in Richmond.

It is likely that domestic fire emissions will continue to be primarily responsible for NES exceedances out to the 2020 full compliance date. When we consider those days that exceeded the New Zealand Ambient Air Quality Guideline (NZAAQG) for $PM_{2.5}$ (25 µg m^{-3}) as shown in Figure 5.7, there were many more days compared to PM_{10} NES exceedances.

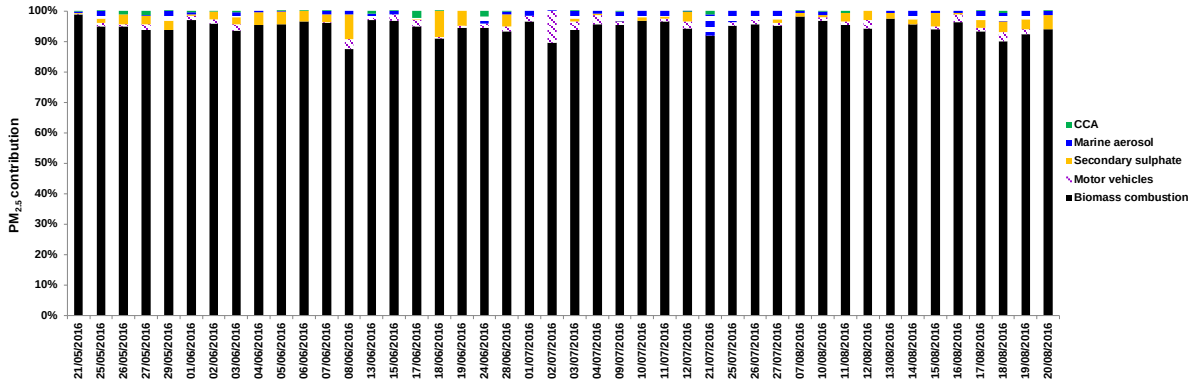

Figure 5.7 Mass contributions to $PM_{2.5}$ exceedance events (> 25 µg m^{-3}) in Richmond.

This result has implications for the health of the exposed population and for air quality management in the Richmond airshed, particularly if a National Environmental Standard for $PM_{2.5}$ (as a 24-hour average) is introduced, since the reduction in particulate matter emissions from biomass combustion sources will have to be significantly greater to achieve compliance.

6.0 SUMMARY OF RICHMOND PARTICULATE MATTER COMPOSITION AND SOURCE CONTRIBUTIONS

A year-long (September 2015 to October 2016) daily $PM_{2.5}$ monitoring and multi-year PM_{10} (June 2013 to October 2016) monitoring programme in Richmond formed the basis of a particulate matter compositional analysis and the attribution of sources contributing to $PM_{2.5}$ and PM_{10} concentrations. The particulate matter elemental composition data showed that black carbon, a product of combustion sources was a dominant contributor to both $PM_{2.5}$ and PM_{10} along with sodium and chlorine which were primarily influenced by marine aerosol (sea salt). The elemental data also showed the influence of pyrotechnics on elements such as potassium, strontium, copper and barium over the Guy Fawkes period (i.e. the days around the 5th November). Elemental arsenic in particulate matter was found to have a general peak in concentrations during winter but also intermittent spikes in concentrations (along with chromium and copper) outside the winter periods in both $PM_{2.5}$ and PM_{10}. It was found that annual average arsenic concentrations in PM_{10} for the 2014 and 2015 calendar years, were 13 (±3) ng m^{-3}, and 16 (±3) ng m^{-3} respectively, significantly higher than the NZAAQG value. The long-term average (2013 to 2016) for arsenic was a similar value (14 ±3 ng m^{-3}).

Five main source types contributing to both $PM_{2.5}$ and PM_{10} were extracted from the data by receptor modelling techniques (using positive matrix factorisation), these were Biomass combustion, Motor vehicles, Secondary sulphate, Marine aerosol and a copper chromium, arsenic (CCA) source. Emissions from biomass combustion, attributed to solid fuel fires for home heating during the winter, were the primary source of both $PM_{2.5}$ and PM_{10} in the Richmond airshed and were also the dominant source contributing to exceedances of the PM_{10} National Environmental Standard for Air Quality (NES) of 50 μg m^{-3}. The data shows that $PM_{2.5}$ dominated PM_{10} concentrations on these days. Arsenic and lead were strongly associated with the Biomass combustion source and this contamination was considered to be from the use of copper chrome arsenate (CCA) treated timber and old painted timber respectively as fuel for domestic fires. A separate source of arsenic associated with chromium and copper was identified as likely to have originated from a local point source northeast of the monitoring site due to the nature of intermittent correlated concentration spikes, typical of an occasional plume touchdown at the Richmond monitoring site depending on wind speed and direction.

It was found that there were many days where $PM_{2.5}$ exceeded the New Zealand Ambient Air Quality (monitoring) Guideline (NZAAQG) of 25 μg m^{-3} compared to PM_{10} NES exceedances. This result has implications for air quality management in the Richmond airshed, particularly if a National Environmental Standard for $PM_{2.5}$ (as a 24-hour average) is introduced, since the reduction in particulate matter emissions from biomass combustion sources will have to be significantly greater to achieve compliance.

7.0 REFERENCES

Ancelet T, Davy PK. 2016. Apportionment of PM10 sources in the Richmond airshed. Lower Hutt (NZ): GNS Science. 49 p. (GNS Science consultancy report; 2016/49).

Ancelet T, Davy PK, Trompetter WJ. 2013. Source apportionment of PM10 and PM2.5 in Nelson Airshed A. Lower Hutt (NZ): GNS Science. (GNS Science consultancy report; 2013/146).

Ancelet T, Davy PK, Mitchell T, Trompetter WJ, Markwitz A, Weatherburn DC. 2012. Identification of particulate matter sources on an hourly time-scale in a wood burning community. *Environmental Science and Technology.* 46(9):4767-4774.

Ancelet T, Davy PK, Trompetter WJ, Markwitz A, Weatherburn DC. 2013. Particulate matter sources on an hourly time-scale in a rural community during the winter. *Journal of the Air & Waste Management Association*. 64(5):501-508.

Ancelet T, Davy PK, Trompetter WJ, Markwitz A, Weatherburn DC. 2014. Sources and transport of particulate matter on an hourly time-scale during the winter in a New Zealand urban valley. *Urban Climate*. 10(P4):644-655.

Anlauf K, Li S-M, Leaitch R, Brook J, Hayden K, Toom-Sauntry D, Wiebe A. 2006. Ionic composition and size characteristics of particles in the Lower Fraser Valley: Pacific 2001 field study. *Atmospheric Environment*. 40(15):2662-2675.

Begum BA, Hopke PK, Zhao WX. 2005. Source identification of fine particles in Washington, DC, by expanded factor analysis modeling. *Environmental Science & Technology*. **39**(4):1129-1137.

Brimblecombe P. 1986. Air: Composition and chemistry. Cambridge (GB): Cambridge University Press.

Brown SG, Eberly S, Paatero P, Norris GA. 2015. Methods for estimating uncertainty in PMF solutions: Examples with ambient air and water quality data and guidance on reporting PMF results. *Science of the Total Environment*. **518-519**:626-635.

Brown SG, Hafner HR. 2005. Multivariate receptor modelling workbook. Petaluma (CA): Sonoma Technology, Inc. Prepared for the U.S. Environmental Protection Agency, Office of Research and Development.

Cahill TA., Eldred RA, Motallebi N, Malm WC. 1989. Indirect measurement of hydrocarbon aerosols across the United States by nonsulfate hydrogen-remaining gravimetric mass correlations. *Aerosol Science and Technology*. **10**(2): 421-429.

Carslaw DC. 2012. The openair manual - open-source tools for analysing air pollution data. Manual for version 0.7-0. London (GB): King's College.

Carslaw DC, Ropkins K. 2012. openair: An R package for air quality data analysis. *Environmental Modelling & Software*. 27-28:52-61.

Chueinta W, Hopke PK, Paatero P. 2000. Investigation of sources of atmospheric aerosol at urban and suburban residential areas in Thailand by positive matrix factorization. *Atmospheric Environment*. 34(20):3319-3329.

Cohen D, Taha G, Stelcer E, Garton D, Box G. 2000. The measurement and sources of fine particle elemental carbon at several key sites in NSW over the past eight years. In: *15th Clean Air Conference*; 2000 Nov 27-30; Sydney, Australia. Mooroolbark (AT): Clean air Society of Australia and New Zealand.

Cohen DD. 1999. Accelerator based ion beam techniques for trace element aerosol analysis. In: Landsberger S, Creatchman M, editors. *Elemental analysis of airborne particles.* Amsterdam (NL): Gordon & Breach. p. 139-196. (Advances in environmental, industrial and process control technologies; 1).

Davy PK. 2007. Composition and sources of aerosol in the Wellington region of New Zealand [PhD thesis]. Wellington (NZ): Victoria University of Wellington. 429 p.

Davy PK, Ancelet T. 2014. Air particulate matter composition, sources and trends in the Whangarei Airshed. Lower Hutt (NZ): GNS Science. 58 p. (GNS Science consultancy report; 2014/186).

Davy PK, Trompetter WJ, Markwitz A. 2009. Source apportionment of airborne particles at Wainuiomata, Lower Hutt. Lower Hutt (NZ): GNS Science. 105 p. (GNS Science consultancy report; 2009/188).

Davy PK, Trompetter WJ, Markwitz A. 2009. Source apportionment of airborne particles in the Auckland region: 2008 update. Lower Hutt (NZ): GNS Science. 439 p. (GNS Science consultancy report; 2009/165).

Davy PK, Trompetter WJ, Markwitz A. 2007. Source apportionment of airborne particles in the Auckland region. Lower Hutt (NZ): GNS Science. 392 p. (GNS Science consultancy report; 2007/314).

Davy PK, Trompetter WJ, Markwitz A. 2008. Source apportionment of airborne particles at Seaview, Lower Hutt. Lower Hutt (NZ): GNS Science. 92 p. (GNS Science consultancy report; 2008/160).

Davy PK, Ancelet A, Trompetter WJ, Markwitz A. 2014. Arsenic and air pollution in New Zealand. In: Litter MI, Nicolli HB, Meichtry M, Quici N, Bundschuh J, Bhattacharya P, Naidu R. *One century of the discovery of arsenicosis in Latin America (1914-2014), As 2014: Proceedings of the 5th International Congress on Arsenic in the Environment*; 2014 May 11-16; Buenos Aires, Argentina. Boca Raton (FL): CRC Press.

Davy PK, Ancelet T, Trompetter WJ, Markwitz A, Weatherburn DC. 2012. Composition and source contributions of air particulate matter pollution in a New Zealand suburban town. *Atmospheric Pollution Research*. 3(1):143-147.

Davy PK, Trompetter WJ, Markwitz A. 2009. Elemental analysis of wood burner emissions. Lower Hutt (NZ): GNS Science. (GNS Science consultancy report; 2009/258).

Davy PK, Trompetter WJ, Markwitz A. 2010. Source apportionment of PM10 at Tahunanui, Nelson. Lower Hutt (NZ): GNS Science. 64 p. (GNS Science consultancy report; 2010/198).

Davy PK, Trompetter WJ, Markwitz A. 2011. Source apportionment of airborne particles in the Auckland region: 2010 analysis. Lower Hutt (NZ): GNS Science. 324 p. GNS Science consultancy report; 2010/262).

Eberly S. 2005. EPA PMF 1.1 User's Guide. Washington (DC): U.S. Environmental Protection Agency.

Fine PM, Cass GR, Simoneit BR. 2001. Chemical characterization of fine particle emissions from fireplace combustion of woods grown in the northeastern United States. *Environmental Science & Technology*. **35**(13):2665-2675.

Gard EE, Kleeman MJ, Gross DS, Hughes LS, Allen JO, Morrical BD, Fergenson DP, Dienes T, Galli ME, Johnson RJ, et al. 1998. Direct observation of heterogeneous chemistry in the atmosphere. *Science*. 279(5354):1184-1187.

George IJ, Abbatt JPD. 2010. Heterogeneous oxidation of atmospheric aerosol particles by gas-phase radicals. *Nature Chemistry*. 2(9):713-722.

Helsen L, van den Bulck E. 2003. Metal retention in the solid residue after low-temperature pyrolysis of Chromated Copper Arsenate (CCA)-treated wood. *Environmental Engineering Science*. 20(6):569-580.

Hopke PK. 1999. An introduction to source receptor modeling. In: Landsberger S, Creatchman M, editors. *Elemental analysis of airborne particles.* Amsterdam (NL): Gordon & Breach. p. 273-315. (Advances in environmental, industrial and process control technologies; 1).

Hopke PK. 2003. Recent developments in receptor modeling. *Journal of Chemometrics*. 17(5):255-265.

Hopke PK, Xie YL, Paatero P. 1999. Mixed multiway analysis of airborne particle composition data. *Journal of Chemometrics.* 13(3-4):343-352.

Horvath H. 1993. Atmospheric light absorption: A review. *Atmospheric Environment. Part A.* 27(3):293-317.

Horvath H. 1997. Experimental calibration for aerosol light absorbtion measurements using the integrating plate method - Summary of the data. *Aerosol Science*. 28:2885-2887.

Jacobson MC, Hansson HC, Noone KJ, Charlson RJ. 2000. Organic atmospheric aerosols: review and state of the science. *Reviews of Geophysics*. 38(2):267-294.

Jeong C-H, Hopke PK, Kim E, Lee D-W. 2004. The comparison between thermal-optical transmittance elemental carbon and Aethalometer black carbon measured at multiple monitoring sites. *Atmospheric Environment*. 38(31):5193.

Kara M, Hopke PK, Dumanoglu Y, Altiok H, Elbir T, Odabasi M, Bayram A. 2015. Characterization of PM using multiple site data in a heavily industrialized region of Turkey. *Aerosol and Air Quality Research*. 15(1):11-27.

Khalil MAK, Rasmussen RA. 2003. Tracers of wood smoke. *Atmospheric Environment*. 37(9-10):1211-1222.

Kim E, Hopke PK, Edgerton ES. 2003. Source identification of Atlanta aerosol by positive matrix factorization. *Journal of the Air & Waste Management Association.* 53(6):731-739.

Kim E, Hopke PK, Larson TV, Maykut NN, Lewtas J. 2004. Factor analysis of Seattle fine particles. *Aerosol Science and Technology.* 38(7):724-738.

Lee E, Chan CK, Paatero P. 1999. Application of positive matrix factorization in source apportionment of particulate pollutants in Hong Kong. *Atmospheric Environment.* 33(19):3201-3212.

Lee JH, Yoshida Y, Turpin BJ, Hopke PK, Poirot RL, Lioy PJ, Oxley JC. 2002. Identification of sources contributing to Mid-Atlantic regional aerosol. *Journal of the Air & Waste Management Association*. 52(10):1186-1205.

Malm WC, Sisler JF, Huffman D, Eldred RA, Cahill TA. 1994. Spatial and seasonal trends in particle concentration and optical extinction in the United States. *Journal of Geophysical Research. Atmospheres.* 99(D1):1347-1370.

New Zealand Ministry for the Environment. 2002. Ambient air quality guidelines. Wellington (NZ): Ministry for the Environment.

O'Dowd CD, Lowe JA, Clegg N, Smith MH Clegg SL. 2000. Modeling heterogeneous sulphate production in maritime stratiform clouds. *Journal of Geophysical Research. Atmospheres.* 105(D6):7143-7160.

Paatero P. 1997. Least squares formulation of robust non-negative factor analysis. *Chemometrics and Intelligent Laboratory Systems.* 18:183-194.

Paatero P. 2000. PMF user's guide. Helsinki (FI): University of Helsinki.

Paatero P, Eberly S, Brown SG, Norris GA. 2014. Methods for estimating uncertainty in factor analytic solutions. *Atmospheric Measurement Techniques.* 7(3):781-797.

Paatero P, Hopke PK. 2002. Utilizing wind direction and wind speed as independent variables in multilinear receptor modeling studies. *Chemometrics and Intelligent Laboratory Systems*. 60(1-2):25-41.

Paatero P, Hopke PK. 2003. Discarding or downweighting high-noise variables in factor analytic models. *Analytica Chimica Acta*. 490(1-2):277-289.

Paatero P, Hopke PK, Begum BA, Biswas SK. 2005. A graphical diagnostic method for assessing the rotation in factor analytical models of atmospheric pollution. *Atmospheric Environment*. 39(1):193-201.

Paatero P, Hopke PK, Song XH, Ramadan Z. 2002. Understanding and controlling rotations in factor analytic models. *Chemometrics and Intelligent Laboratory Systems*. 60(1-2):253-264.

Ramadan Z, Eickhout B, Song X-H, Buydens LMC, Hopke PK. 2003. Comparison of positive matrix factorization and multilinear engine for the source apportionment of particulate pollutants. *Chemometrics and Intelligent Laboratory Systems*. 66(1):15-28.

Salma I, Chi X, Maenhaut W. 2004. Elemental and organic carbon in urban canyon and background environments in Budapest, Hungary. *Atmospheric Environment.* 38(1):27-36.

Scott AJ. 2006. Source apportionment and chemical characterisation of airborne fine particulate matter in Christchurch, New Zealand. [PhD thesis]. Christchurch (NZ): University of Canterbury.

Seinfeld JH, Pandis SN. 2006. Atmospheric chemistry and physics: From air pollution to climate change. New York (NY): John Wiley & Sons, Inc.

Song XH, Polissar AV, Hopke PK. 2001. Sources of fine particle composition in the northeastern US. *Atmospheric Environment*. 35(31):5277-5286.

Team RDC. 2011. R: A language and environment for statistical computing. Vienna (AT): R Foundation for Statistical Computing.

Trompetter WJ. 2004. Ion Beam Analysis results of air particulate filters from the Wellington Regional Council. Lower Hutt (NZ): Institute of Geological & Nuclear Sciences. 17 p. (Institute of Geological & Nuclear Sciences client report; 2004/24).

Watson JG, Chow JC, Frazier CA. 1999. X-ray fluorescence analysis of ambient air samples. In: Landsberger S, Creatchman M, editors. *Elemental analysis of airborne particles.* Amsterdam (NL): Gordon & Breach. p. 67-96. (Advances in environmental, industrial and process control technologies; 1).

Watson JG, Zhu T, Chow JC, Engelbrecht J, Fujita EM, Wilson WE. 2002. Receptor modeling application framework for particle source apportionment. *Chemosphere*. 49(9):1093-1136.

APPENDICES

A1.0 ANALYSIS TECHNIQUES

A1.1 X-RAY FLUORESCENCE SPECTROSCOPY (XRF)

X-ray fluorescence spectroscopy (XRF) was used to measure elemental concentrations in $PM_{2.5}$ and PM_{10} samples collected on Teflon filters in Richmond. XRF measurements in this study were carried out at the GNS Science XRF facility and the spectrometer used was a PANalytical Epsilon 5 (PANalytical, the Netherlands). The Epsilon 5 is shown in Figure A1.1. XRF is a non-destructive and relatively rapid method for the elemental analysis of particulate matter samples.

Figure A1.1 The PANalytical Epsilon 5 spectrometer.

XRF is based on the measurement of characteristic X-rays produced by the ejection of an inner shell electron from an atom in the sample, creating a vacancy in the inner atomic shell. A higher energy electron then drops into the lower energy orbital and releases a fluorescent X-ray to remove excess energy (Watson, Chow et al. 1999). The energy of the released X-ray is characteristic of the emitting element and the area of the fluorescent X-ray peak (intensity of the peak) is proportional to the number of emitting atoms in the sample. From the intensity it is possible to calculate a specific element's concentration by direct comparison with standards.

To eject inner shell electrons from atoms in a sample, XRF spectrometer at GNS Science uses a 100 kV Sc/W X-ray tube. The 100 kV X-rays produced by this tube are able to provide elemental information for elements from Na–U. Unlike ion beam analysis techniques, which are similar to XRF, the PANalytical Epsilon 5 is able to use characteristic K-lines produced by each element for quantification. This is crucial for optimising limits of detection because K-lines

have higher intensities and are located in less crowded regions of the X-ray spectrum. The X-rays emitted by the sample are detected using a high performance Ge detector, which further improves the detection limits. Figure A1.2 presents a sample X-ray spectrum.

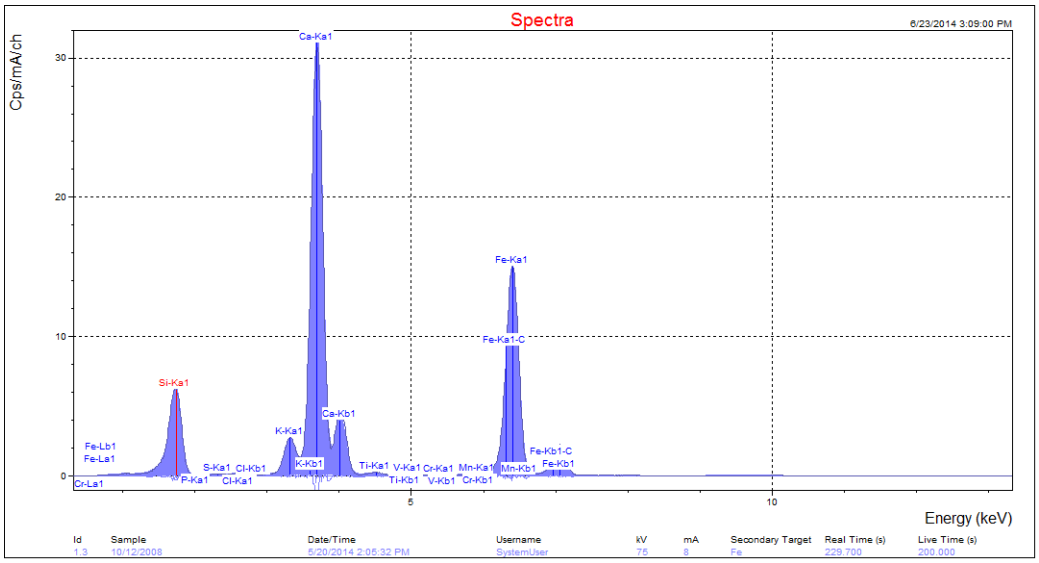

Figure A1.2 Example X-ray spectrum from a PM_{10} sample.

In this study, calibration standards for each of the elements of interest were analysed prior to the samples being run. Once the calibration standards were analysed, spectral deconvolutions were performed using PANalytical software to correct for line overlaps and ensure that the spectra were accurately fit. Calibration curves for each element of interest were produced and used to determine the elemental concentrations from the Richmond samples. A NIST reference sample was also analysed to ensure that the results obtained were robust and accurate.

A1.2 BLACK CARBON MEASUREMENTS

Black carbon (BC) has been studied extensively, but it is still not clear to what degree it is elemental carbon (EC (or graphitic) C(0)) or high molecular weight refractory weight organic species or a combination of both (Jacobson, Hansson et al. 2000). Current literature suggests that BC is likely a combination of both, and that for combustion sources such as petrol and diesel fuelled vehicles and biomass combustion (wood burning, coal burning), EC and organic carbon compounds (OC) are the principle aerosol components emitted (Jacobson, Hansson et al. 2000, Fine, Cass et al. 2001, Watson, Zhu et al. 2002, Salma, Chi et al. 2004).

Determination of carbon (soot) on filters was performed by light reflection to provide the BC concentration. The absorption and reflection of visible light on particles in the atmosphere or collected on filters is dependent on the particle concentration, density, refractive index and size. For atmospheric particles, BC is the most highly absorbing component in the visible light spectrum with very much smaller components coming from soils, sulphates and nitrate (Horvath 1993, Horvath 1997). Hence, to the first order it can be assumed that all the absorption on atmospheric filters is due to BC. The main sources of atmospheric BC are anthropogenic combustion sources and include biomass burning, motor vehicles and industrial emissions (Cohen, Taha et al. 2000). Cohen and co-workers found that BC is typically 10 – 40 % of the fine mass ($PM_{2.5}$) fraction in many urban areas of Australia.

When measuring BC by light reflection/transmission, light from a light source is transmitted through a filter onto a photocell. The amount of light absorption is proportional to the amount of black carbon present and provides a value that is a measure of the black carbon on the filter. Conversion of the absorbance value to an atmospheric concentration value of BC requires the use of an empirically derived equation (Cohen, Taha et al. 2000):

$$BC\ (\mu g\ cm^{-2}) = (100/2(F\varepsilon))\ \ln[R_0/R] \qquad (A1.1)$$

where:

ε is the mass absorbent coefficient for BC ($m^2\ g^{-1}$) at a given wavelength;

F is a correction factor to account for other absorbing factors such as sulphates, nitrates, shadowing and filter loading. These effects are generally assumed to be negligible and F is set at 1.00;

R_0, R are the pre- and post-reflection intensity measurements, respectively.

Black carbon was measured at GNS Science using the M43D Digital Smoke Stain Reflectometer. The following equation (from Willy Maenhaut, Institute for Nuclear Sciences, University of Gent Proeftuinstraat 86, B-9000 GENT, Belgium) was used for obtaining BC from reflectance measurements on Nucleopore polycarbonate filters or Pall Life Sciences Teflon filters:

$$BC\ (\mu g\ cm^{-2}) = [1000 \times LOG(R_{blank}/R_{sample}) + 2.39] / 45.8 \qquad (A1.2)$$

where:

R_{blank}: the average reflectance for a series of blank filters; R_{blank} is close (but not identical) to 100. GNS always use the same blank filter for adjusting to 100.

R_{sample}: the reflectance for a filter sample (normally lower than 100).

With: 2.39 and 45.8 constants derived using a series of 100 Nuclepore polycarbonate filter samples which served as secondary standards; the BC loading (in µg cm^{-2}) for these samples had been determined by Prof. Dr. M.O. Andreae (Max Planck Institute of Chemistry, Mainz, Germany) relative to standards that were prepared by collecting burning acetylene soot on filters and determining the mass concentration gravimetrically (Trompetter 2004).

A1.3 POSITIVE MATRIX FACTORIZATION

Positive matrix factorisation (PMF) is a linear least-squares approach to factor analysis and was designed to overcome the receptor modeling problems associated with techniques like principal components analysis (PCA) (Paatero, Hopke et al. 2005). With PMF, sources are constrained to have non-negative species concentrations, no sample can have a negative source contribution and error estimates for each observed data point are used as point-by-point weights. This feature is a distinct advantage, in that it can accommodate missing and below detection limit data that is a common feature of environmental monitoring results (Song, Polissar et al. 2001). In fact, the signal to noise ratio for an individual elemental measurement can have a significant influence on a receptor model and modeling results. For the weakest (closest to detection limit) species, the variance may be entirely from noise (Paatero and Hopke 2002). Paatero and Hopke strongly suggest down-weighting or discarding noisy variables that are always below their detection limit or species that have a lot of error in their measurements relative to the magnitude of their concentrations (Paatero and Hopke 2003). The distinct advantage of PMF is that mass concentrations can be included in the model and the results are directly interpretable as mass contributions from each factor (source).

A1.3.1 PMF Model Outline

The mathematical basis for PMF is described in detail by Paatero (Paatero 1997, Paatero 2000). Briefly, PMF uses a weighted least-squares fit with the known error estimates of measured elemental concentrations used to derive the weights. In matrix notation this is indicated as:

$$X = GF + E \tag{A1.3}$$

where:

X is the known *n* x *m* matrix of *m* measured elemental species in *n* samples;

G is an *n* x *p* matrix of source contributions to the samples;

F is a *p* x *m* matrix of source compositions (source profiles).

E is a residual matrix – the difference between measurement *X* and model *Y.*

E can be defined as a function of factors *G* and *F*:

$$e_{ij} = x_{ij} - y_{ij} = x_{ij} - \sum_{k=1}^{p} g_{ik} f_{kj} \tag{A1.4}$$

where:

i = 1,……,*n* elements

j = 1,……,*m* samples

k = 1,…...,*p* sources

PMF constrains all elements of *G* and *F* to be non-negative, meaning that elements cannot have negative concentrations and samples cannot have negative source contributions as in real space. The task of PMF is to minimise the function *Q* such that:

$$Q(E) = \sum_{i=1}^{n} \sum_{j=1}^{m} (e_{ik} / \sigma_{kj})^2 \quad \text{(A1.5)}$$

where σ_{ij} is the error estimate for x_{ij}. Another advantage of PMF is the ability to handle extreme values typical of air pollutant concentrations as well as true outliers that would normally skew PCA. In either case, such high values would have significant influence on the solution (commonly referred to as leverage). PMF has been successfully applied to receptor modeling studies in a number of countries around the world (Hopke, Xie et al. 1999, Lee, Chan et al. 1999, Chueinta, Hopke et al. 2000, Song, Polissar et al. 2001, Lee, Yoshida et al. 2002, Kim, Hopke et al. 2003, Jeong, Hopke et al. 2004, Kim, Hopke et al. 2004, Begum, Hopke et al. 2005) including New Zealand (Scott 2006, Davy 2007, Davy, Trompetter et al. 2007, Davy, Trompetter et al. 2008, Davy, Trompetter et al. 2009, Davy, Trompetter et al. 2009, Ancelet, Davy et al. 2012).

A1.3.2 PMF Model Used

Two programs have been written to implement different algorithms for solving the least squares PMF problem, these are PMF2 and EPAPMF, which incorporates the Multilinear Engine (ME-2) (Hopke, Xie et al. 1999, Ramadan, Eickhout et al. 2003). In effect, the EPAPMF program provides a more flexible framework than PMF2 for controlling the solutions of the factor analysis with the ability of imposing explicit external constraints.

This study used EPAPMF 5.0 (version 14.1.3), which incorporates a graphical user interface (GUI) based on the ME-2 program. Both PMF2 and EPAPMF programs can be operated in a robust mode, meaning that “outliers” are not allowed to overly influence the fitting of the contributions and profiles (Eberly 2005). The user specifies two input files, one file with the concentrations and one with the uncertainties associated with those concentrations. The methodology for developing an uncertainty matrix associated with the elemental concentrations for this work is discussed in Section A1.4.2.

A1.3.3 PMF Model Inputs

The PMF programs provide the user with a number of choices in model parameters that can influence the final solution. Two parameters, the ‘signal-to-noise ratio’ and the ‘species category’ are of particular importance and are described below.

Signal-to-noise ratio - this is a useful diagnostic statistic estimated from the input data and uncertainty files using the following calculation:

$$(1/2) \sqrt{\sum_{i=1}^{n} (x_{ij})^2 / \sum_{i=1}^{n} (\sigma_{ij})^2} \quad \text{(A1.6)}$$

Where x_{ij} and σ_{ij} are the concentration and uncertainty, respectively, of the i^{th} element in the j^{th} sample. Smaller signal-to-noise ratios indicate that the measured elemental concentrations are generally near the detection limit and the user should consider whether to include that species in the receptor model or at least strongly down-weight it (Paatero and Hopke 2003). The signal-to-noise ratios (S/N ratio) for each element are reported alongside other statistical data in the results section.

Species category - this enables the user to specify whether the elemental species should be considered:

- Strong – whereby the element is generally present in concentrations well above the LOD (high signal to noise ratio) and the uncertainty matrix is a reasonable representation of the errors.
- Weak – where the element may be present in concentrations near the LOD (low signal to noise ratio); there is doubt about some of the measurements and/or the error estimates; or the elemental species is only detected some of the time. If 'Weak' is chosen EPA.PMF increases the user-provided uncertainties for that variable by a factor of 3.
- Bad – that variable is excluded from the model run.

For this work, an element with concentrations at least 3 times above the LOD, a high signal to noise ratio (> 2) and present in all samples was considered 'Strong'. Variables were labelled as weak if their concentrations were generally low, had a low signal to noise ratio, were only present in a few samples or there was a lower level of confidence in their measurement. Mass concentration gravimetric measurements and BC were also down weighted as 'Weak' because their concentrations are generally several orders of magnitude above other species, which can have the tendency to 'pull' the model. Paatero and Hopke recommend that such variables be down weighted and that it doesn't particularly affect the model fitting if those variables are from real sources (Paatero and Hopke 2003). What does affect the model severely is if a dubious variable is over-weighted. Elements that had a low signal to noise ratio (< 0.2), or had mostly missing (zero) values, or were doubtful for any reason, were labelled as 'Bad' and were subsequently not included in the analyses.

If the model is appropriate for the data and if the uncertainties specified are truly reflective of the uncertainties in the data, then *Q* (according to Eberly) should be approximately equal to the number of data points in the concentration data set (Eberly 2005):

$$\textit{Theoretical } Q = \#\textit{ samples } \mathbf{x} \#\textit{ species measured} \quad \text{(A1.7)}$$

However, a slightly different approach to calculating the Theoretical *Q* value was recommended by (Brown and Hafner 2005), which takes into account the degrees of freedom in the PMF model and the additional constraints in place for each model run. This theoretical *Q* calculation Q_{th} is given as:

$$Q_{th} = (\#\textit{ samples } \mathbf{x} \#\textit{ good species}) + [(\#\textit{ samples } \mathbf{x} \#\textit{ weak species})/3] - (\#\textit{ samples } \mathbf{x}\textit{ factors estimated}) \quad \text{(A1.8)}$$

Both approaches have been taken into account for this study and it is likely that the actual value lies somewhere between the two.

In PMF, it is assumed that only the x_{ij}'s are known and that the goal is to estimate the contributions (g_{ik}) and the factors (or profiles) (f_{kj}). It is assumed that the contributions and mass fractions are all non-negative, hence the "constrained" part of the least-squares. Additionally, EPAPMF allows the user to say how much uncertainty there is in each x_{ij}. Species-days with lots of uncertainty are not allowed to influence the estimation of the contributions and profiles as much as those with small uncertainty, hence the "weighted" part of the least squares and the advantage of this approach over PCA.

Diagnostic outputs from the PMF models were used to guide the appropriateness of the number of factors generated and how well the receptor modelling was accounting for the input data. Where necessary, initial solutions have been ‘rotated’ to provide a better separation of factors (sources) that were considered physically reasonable (Paatero, Hopke et al. 2002). Each PMF model run reported in this study is accompanied by the modelling statistics along with comments where appropriate.

A1.4 DATASET QUALITY ASSURANCE

Quality assurance of sample elemental datasets is vital so that any dubious samples, measurements and outliers are removed as these will invariably affect the results of receptor modelling. In general, the larger the dataset used for receptor modelling, the more robust the analysis. The following sections describe the methodology used to check data integrity and provide a quality assurance process that ensured that the data being used in subsequent factor analysis was as robust as possible.

A1.4.1 Mass Reconstruction and Mass Closure

Once the sample analysis for the range of analytes has been carried out, it is important to check that total measured mass does not exceed gravimetric mass (Cohen 1999). Ideally, when elemental analysis and organic compound analysis has been undertaken on the same sample one can reconstruct the mass using the following general equation for ambient samples as a first approximation (Cahill, Eldred et al. 1989, Malm, Sisler et al. 1994, Cohen 1999):

$$\text{Reconstructed mass} = [\text{Soil}] + [\text{BC}] + [\text{Smoke}] + [\text{Sulphate}] + [\text{Seasalt}] \quad \text{(A1.9)}$$

where:

[Soil] = 2.20[Al] + 2.49[Si] + 1.63[Ca] + 2.42[Fe] + 1.94[Ti]

[BC] = Concentration of black carbon (soot)

[Smoke] = [K] − 0.6[Fe]

[Seasalt] = 2.54[Na]

[Sulphate] = 4.125[S]

The reconstructed mass (RCM) is based on the fact that the six composite variables or ‘pseudo’ sources given in equation A1.9 are generally the major contributors to fine and coarse particle mass and are based on geochemical principles and constraints. The [Soil] factor contains elements predominantly found crustal matter (Al, Si, Ca, Fe, Ti) and includes a multiplier to correct for oxygen content and an additional multiplier of 1.16 to correct for the fact that three major oxide contributors (MgO, K_2O, Na_2O) carbonate and bound water are excluded from the equation.

[BC] is the concentration of black carbon, measured in this case by light reflectance/absorbance. [Smoke] represents K not included as part of crustal matter and tends to be an indicator of biomass burning.

[Seasalt] represents the marine aerosol contribution and assumes that the NaCl weight is 2.54 times the Na concentration. Na is used as it is well known that Cl can be volatilised from aerosol or from filters in the presence of acidic aerosol, particularly in the fine fraction via the following reactions (Lee, Chan et al. 1999):

$$NaCl(p) + HNO_3(ag) \rightarrow NaNO_3(p) + HCL(g) \quad \text{(A1.10)}$$

$$2NaCl(p) + H_2SO_4(ag) \rightarrow Na_2SO_4(p) + 2HCL(g) \quad \text{(A1.11)}$$

Alternatively, where Cl loss is likely to be minimal, such as in the coarse fraction or for both size fractions near coastal locations and relatively clean air in the absence of acid aerosol, then the reciprocal calculation of [Seasalt] = 1.65[Cl] can be substituted, particularly where Na concentrations are uncertain.

Most fine sulphate particles are the result of oxidation of SO_2 gas to sulphate particles in the atmosphere (Malm, Sisler et al. 1994). It is assumed that sulphate is present in fully neutralised form as ammonium sulphate. [Sulphate] therefore represents the ammonium sulphate contribution to aerosol mass with the multiplicative factor of 4.125[S] to account for ammonium ion and oxygen mass (i.e. $(NH_4)_2SO_4$ = ((14 + 4)2 + 32 + (16x4)/32)).

Additionally, the sulphate component not associated with seasalt can be calculated from equation A1.13 (Cohen 1999):

$$\text{Non-seasalt sulphate (NSS-Sulphate)} = 4.125\ ([S_{tot}] - 0.0543[Cl]) \qquad \text{(A1.12)}$$

Where the sulphur concentrations contributed by seasalt are inferred from the chlorine concentrations, i.e. [S/Cl]seasalt = 0.0543 and the factor of 4.125 assumes that the sulphate has been fully neutralised and is generally present as $(NH_4)_2SO_4$ (Cahill, Eldred *et al*. 1990; Malm, Sisler *et al*. 1994; Cohen 1999).

The RCM and mass closure calculations using the pseudo-source and pseudo-element approach are a useful way to examine initial relationships in the data and how the measured mass of species in samples compares to gravimetric mass. Note that some scatter is possible because not all aerosols are necessarily measured and accounted for, such as all OC, ammonium species, nitrates and unbound water.

As a quality assurance mechanism, those samples for which RCM exceeded gravimetric mass or where gravimetric mass was significantly higher than RCM were examined closely to assess gravimetric mass and XRF data. Where there was significant doubt either way, those samples were excluded from the receptor modeling analysis. The reconstructed mass calculations and pseudo source estimations are presented in the appendices at the end of this report.

A1.4.2 Dataset Preparation

Careful preparation of a dataset is required because serious errors in data analysis and receptor modeling results can be caused by erroneous individual data values. The general methodology followed for dataset preparation was as recommended by (Brown and Hafner 2005). For this study, all data were checked for consistency with the following parameters:

1. Individual sample collection validation;
2. Gravimetric mass validation;
3. Analysis of RCM versus gravimetric mass to ensure RCM < gravimetric;
4. Identification of unusual values including noticeably extreme values and values that normally track with other species (e.g. Al and Si) but deviate in one or two samples. Scatter plots and time series plots were used to identify unusual values. One-off events such as fireworks displays, forest fires or vegetative burn-offs may affect a receptor model as it is forced to find a profile that matches only that day;

5. Species were included in a dataset if at least 70 % of data was above the LOD and signal-to-noise ratios were checked to ensure data had sufficient variability. Important tracers of a source where less than 70 % of data was above the LOD were included but model runs with and without the data were used to assess the effect;

In practice during data analyses, the above steps were a reiterative process of cross checking as issues were identified and corrected for, or certain data excluded and the effects of this were then studied.

The following steps were followed to produce a final dataset for use in the PMF receptor model (Brown and Hafner 2005).

Below detection limit data: For given values, the reported concentration used and the corresponding uncertainty checked to ensure it had a high value.

Missing data: Substituted with the dataset median value for that species.

Uncertainties can have a large effect on model results so that they must be carefully compiled. The effect of underestimating uncertainties can be severe, while overestimating uncertainties does not do too much harm (Paatero and Hopke 2003).

Uncertainties for data: Uncertainties for the XRF elemental data were calculated using the following equations (Kara, Hopke et al. 2015):

$\sigma_{ij} = x_{ij} + 2/3(DL_j)$ for samples below limit of detection;

$\sigma_{ij} = 0.2x_{ij} + 2/3(DLj)$; $DL_j < x_{ij} < 3DL_j$ and $\sigma_{ij} = 0.1x_{ij} + 2/3(DL_j)$; $x_{ij} > 3DL_j$: for detected values

where x_{ij} is the determined concentration for species j in the ith sample, and DL_j is the detection limit for species j.

Below detection limit data: Below detection limit data was generally provided with a high % fit error and this was used to produce an uncertainty in ng m^{-3}.

Missing data: Uncertainty was calculated as 4 × median value over the entire species dataset.

PM gravimetric mass: Uncertainty given as 4 × mass value to down-weight the variable.

Reiterative model runs were used to examine the effect of including species with high uncertainties or low concentrations. In general, it was found that the initial uncertainty estimations were sufficient and that adjusting the ‘additional modelling uncertainty’ function accommodated any issues with modelled variables such as those with residuals outside ± 3 standard deviations.

A2.0 RICHMOND $PM_{2.5}$ AND PM_{10} DATA ANALYSIS SUMMARY

Using the methodology outlined in Section A1.4.1, Figures A2.1 and A2.2 present the mass reconstruction results for Richmond $PM_{2.5}$ and PM_{10} respectively. Figures A2.4 and A2.5 present correlation plot matrices for key elemental species in $PM_{2.5}$ and PM_{10} respectively. The deviation in linearity at higher concentrations evident in Figures A2.1 and A2.2 is due to the influence of unmeasured PM components on mass composition. Since the PMF receptor modelling process is an analysis of variance and covariance, such deviation only becomes a problem if those unmeasured species are not covariant with at least some of the measured species – in this case potassium and black carbon are clearly covariant with PM_{10} at high concentrations as shown in Figure A2.2. Since biomass combustion dominates higher PM_{10} concentrations in Richmond, the unmeasured mass was the hydrocarbon aerosol associated with incomplete combustion of wood. The hydrocarbon aerosol from the pyrolysis of wood has been shown to be approximately 90% of the particulate mass emissions from woodburners (Davy, Trompetter et al. 2009). A critical factor in the success of receptor modelling is the ability to reproduce observed versus predicted (modelled) mass. This was clearly being achieved in the case of Richmond $PM_{2.5}$ (and PM_{10}) as presented in Figures A2.6 and A2.7 respectively showing observed versus predicted (modelled) mass.

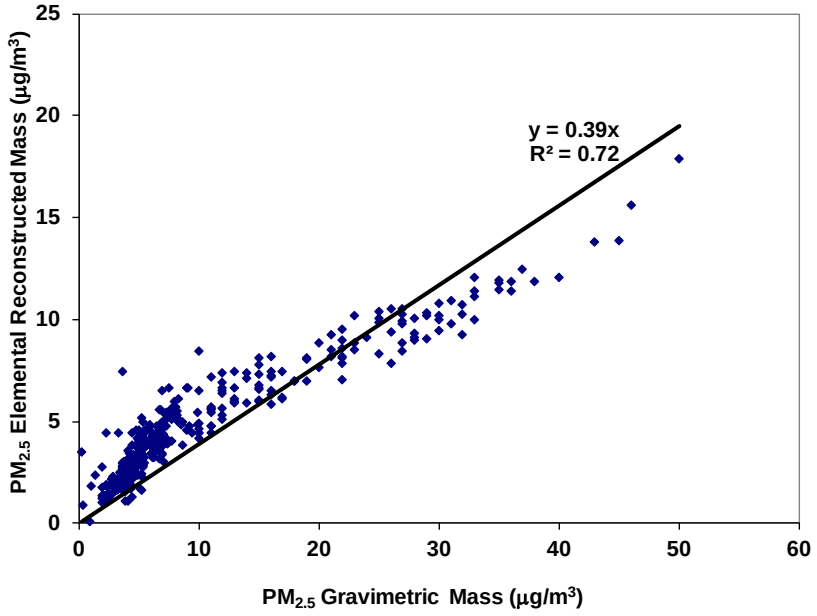

Figure A2.1 Plot of Richmond $PM_{2.5}$ elemental mass reconstruction against gravimetric $PM_{2.5}$ mass.

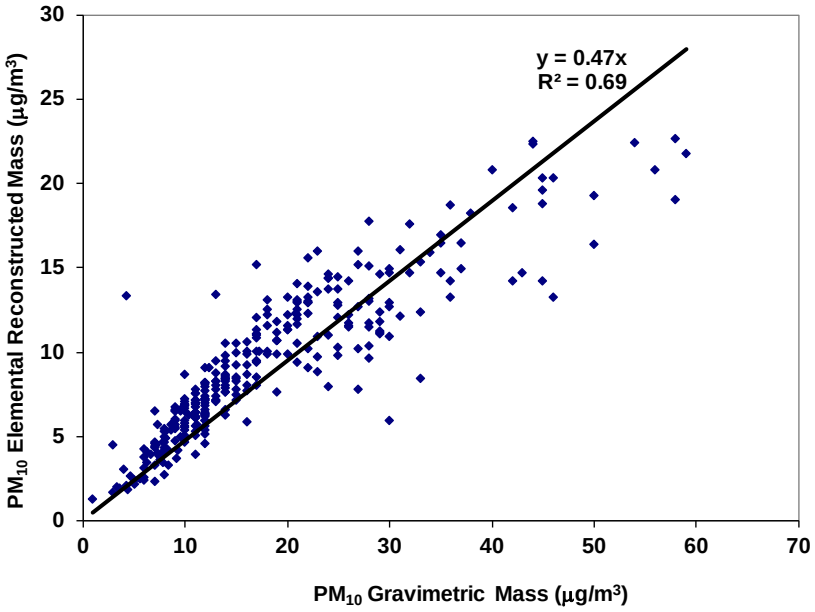

Figure A2.2 Plot of Richmond PM_{10} elemental mass reconstruction against gravimetric PM_{10} mass.

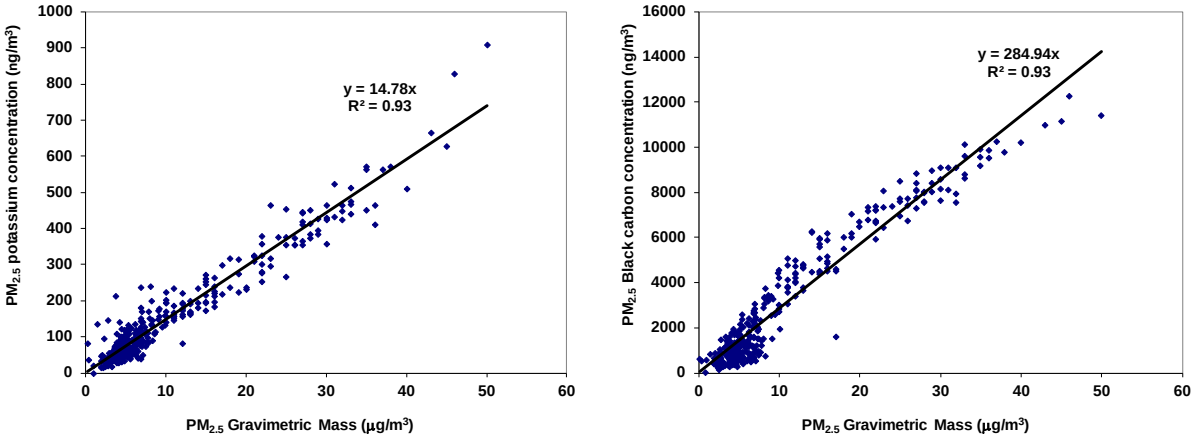

Figure A2.3 Plot of Richmond $PM_{2.5}$ potassium elemental (left) and black carbon mass (right) against $PM_{2.5}$ gravimetric mass.

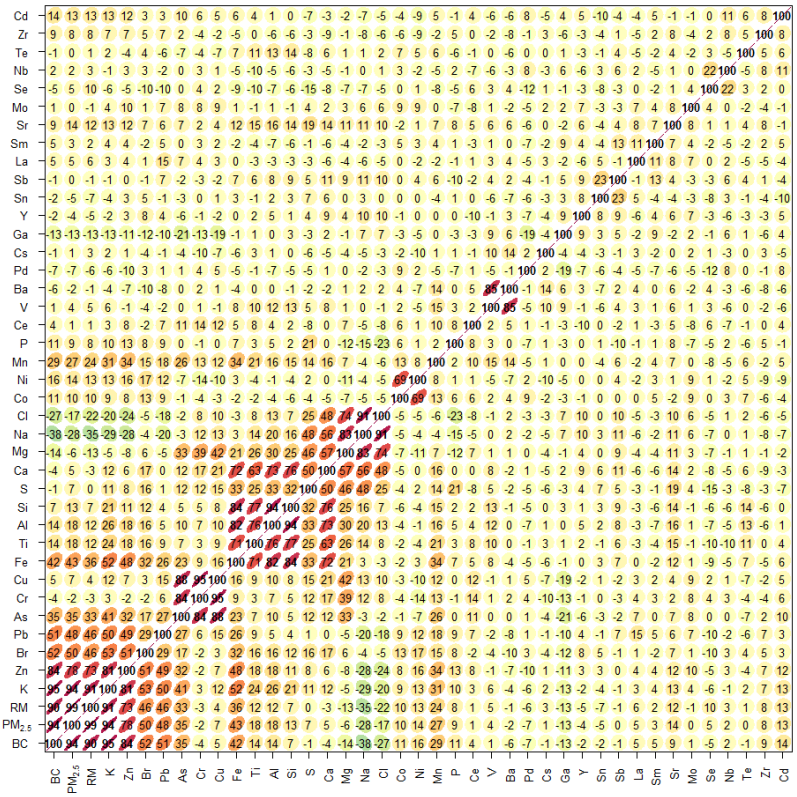

Figure A2.4 Richmond $PM_{2.5}$ elemental correlation plot.

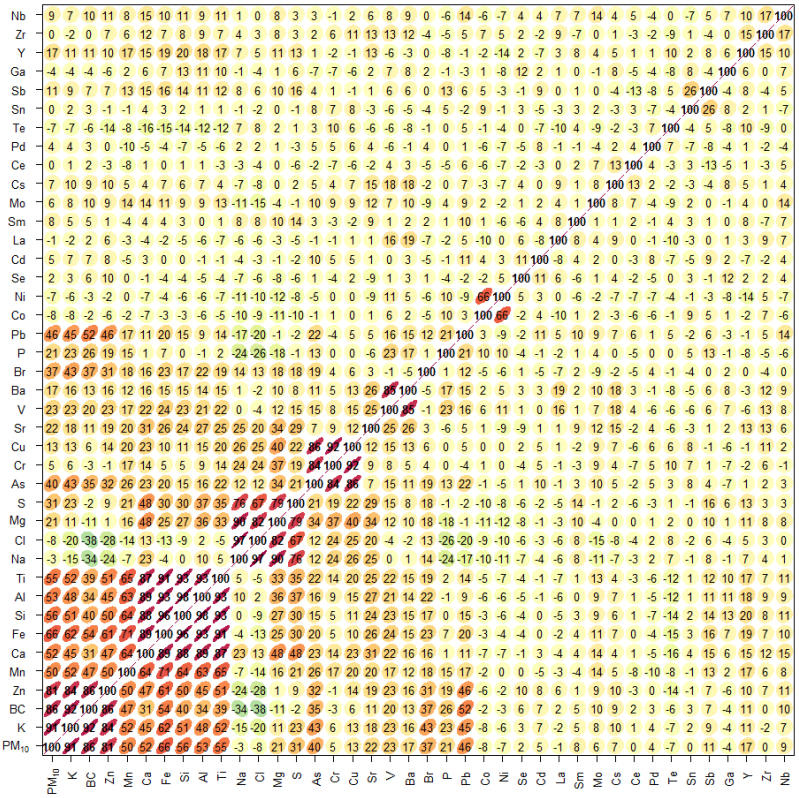

Figure A2.5 Richmond PM_{10} Elemental correlation plot.

A2.1 RICHMOND $PM_{2.5}$ AND PM_{10} PMF RECEPTOR MODELLING DIAGNOSTICS

PMF analyses involve many details about the development of the data, decisions of what data to include/exclude, determination of a solution, and evaluation of robustness of that solution. The following diagnostics for the PMF solutions are reported as recommended by Paatero and co-workers (Paatero, Eberly et al. 2014, Brown, Eberly et al. 2015) and should be read in conjunction with Section 2.1 and Appendix 1.

Summary of EPA PMF settings for receptor modelling of Richmond $PM_{2.5}$

Parameter	Setting
Data type; averaging timeframe	$PM_{2.5}$, Daily
N samples	356
N factors	5
Treatment of missing data	No missing data
Treatment of data below detection limit (BDL)	Data used as reported, no modification or censoring of BDL data
Lower limit for normalized factor contributions gik	-0.2
Robust mode	Yes
Constraints	None
Seed value	Random
N bootstraps in BS	200
r2 for BS	0.6
DISP dQmax	4, 8, 16, 32
DISP active species	$PM_{2.5}$, Si, S, K, Ca, Cr, Fe, Cu, Zn, As
N bootstraps; r2 for BS in BS-DISP	200; 0.6
BS-DISP active species	Si, S, K, Ca, Cr, Fe, Cu, Zn, As
BS-DISP dQmax	0.5, 1, 2, 4
Extra modelling uncertainty	0%

Output diagnostics for receptor modelling of Richmond $PM_{2.5}$

Diagnostic	5 Factors
$Q_{Theoretical}$	2443
$Q_{Expected}$	1695
Q_{true}	1995.89
Q_{robust}	1963.08
$Q_{robust}/Q_{expected}$	1.178
DISP Diagnostics:	
Error code	0
Largest decrease	0
DISP % dQ	0
DISP swaps by factor	0
BS-DISP Diagnostics:	
BS mapping (Fpeak BS) - Unmapped	99.7% (100%) - 0
BS-DISP % cases accepted	98%
Largest Decrease in Q:	-33.8
BS-DISP % dQ	-1.72
# of Decreases in Q:	2
# of Swaps in Best Fit:	1
# of Swaps in DISP:	0
BS-DISP swaps by factor	1,0,0,0,1

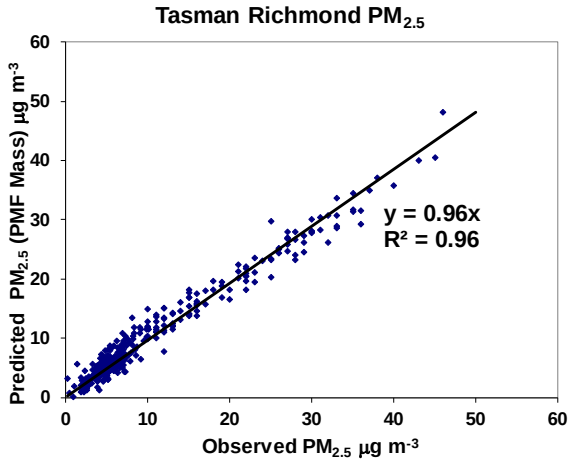

Figure A2.6 Plot of Richmond PM_{10} predicted (PMF mass) against observed gravimetric PM_{10} mass.

Summary of EPA PMF settings for receptor modelling of Richmond PM_{10}

Parameter	Setting
Data type; averaging timeframe	PM_{10}, Daily
N samples	313
N factors	5
Treatment of missing data	No missing data
Treatment of data below detection limit (BDL)	Data used as reported, no modification or censoring of BDL data
Lower limit for normalized factor contributions gik	-0.2
Robust mode	Yes
Constraints	None
Seed value	Random
N bootstraps in BS	200
r^2 for BS	0.6
DISP dQmax	4, 8, 16, 32
DISP active species	PM_{10}, BC, Na, Al, Si, S, Cl, K, Ca, Ti, Cr, Mn, Fe, Cu, Zn, As
N bootstraps; r^2 for BS in BS-DISP	200; 0.6
BS-DISP active species	Si, S, K, Ca, Cr, Fe, Cu, Zn, As
BS-DISP dQmax	0.5, 1, 2, 4
Extra modelling uncertainty	10%

Output diagnostics for receptor modelling of Richmond PM_{10}

Diagnostic	5 Factors
$Q_{Theoretical}$	3652
$Q_{Expected}$	3363
Q_{true}	1828.19
Q_{robust}	1830.11
$Q_{robust}/Q_{expected}$	0.544
DISP Diagnostics:	
Error code	0
Largest decrease	0
DISP % dQ	0
DISP swaps by factor	0
BS-DISP Diagnostics:	
BS mapping (Fpeak BS) - Unmapped	95% (96%) - 0
BS-DISP % cases accepted	94%
Largest Decrease in Q:	-10.2
BS-DISP % dQ	-0.556
# of Decreases in Q:	0
# of Swaps in Best Fit:	4
# of Swaps in DISP:	9
BS-DISP swaps by factor	6,2,4,0,2

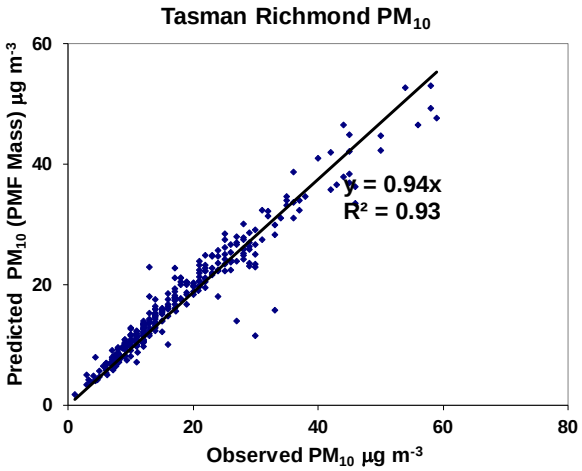

Figure A2.7 Plot of Richmond PM_{10} predicted (PMF mass) against observed PM_{10} mass.

www.gns.cri.nz

Principal Location

1 Fairway Drive
Avalon
PO Box 30368
Lower Hutt
New Zealand
T +64-4-570 1444
F +64-4-570 4600

Other Locations

Dunedin Research Centre
764 Cumberland Street
Private Bag 1930
Dunedin
New Zealand
T +64-3-477 4050
F +64-3-477 5232

Wairakei Research Centre
114 Karetoto Road
Wairakei
Private Bag 2000, Taupo
New Zealand
T +64-7-374 8211
F +64-7-374 8199

National Isotope Centre
30 Gracefield Road
PO Box 31312
Lower Hutt
New Zealand
T +64-4-570 1444
F +64-4-570 4657